CHEMICAL REVIEWS

Review

pubs.acs.org/CR

Advances in Plasmonic Technologies for Point of Care Applications

Onur Tokel,[†,⊥] Fatih Inci,[†,∥] and Utkan Demirci*[,†,‡,§,∥]

[†]Demirci Bio-Acoustic-MEMS in Medicine (BAMM) Laboratory, Department of Medicine, Brigham and Women's Hospital, Harvard Medical School, Cambridge, Massachusetts 02139, United States

[‡]Division of Infectious Diseases, Brigham and Women's Hospital, Harvard Medical School, Boston, Massachusetts 02115, United States

[§]Harvard-MIT Health Sciences and Technology, Cambridge, Massachusetts 02139, United States

[∥]Demirci Bio-Acoustic-MEMS in Medicine (BAMM) Laboratory, Stanford University School of Medicine, Canary Center at Stanford for Cancer Early Detection, Palo Alto, California 94304, United States

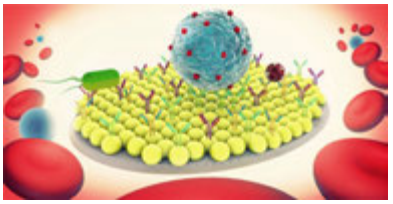

CONTENTS

1. INTRODUCTION

Demand for accessible and affordable healthcare for infectious and chronic diseases present significant challenges for providing high-value and effective healthcare. Traditional approaches are expanding to include point-of-care (POC) diagnostics, bedside testing, and community-based approaches to respond to these challenges.[1] Innovative solutions utilizing recent advances in mobile technologies, nanotechnology, imaging systems, and microfluidic technologies are envisioned to assist this transformation.

Infectious diseases have considerable economic and societal impact on developing settings. For instance, malaria is observed more commonly in sub-Saharan Africa and India.[2] The societal impact of acquired immune deficiency syndrome (AIDS) and tuberculosis is high, through targeting adults in villages and leaving behind declining populations.[3] In resource-constrained settings, it is estimated that about 32% of the disease burden is from communicable diseases such as respiratory infections, AIDS, and malaria, while 43% of the burden is from noncommunicable diseases, such as cardiovascular diseases, neuropsychiatric conditions, and cancer.[4] Developing diagnostic platforms that are affordable, robust, and rapid-targeting infectious diseases is one of the top priorities for improving healthcare delivery in the developing world.[5] The early detection and monitoring of infectious diseases and cancer through affordable and accessible healthcare will significantly reduce the disease burden and help preserve the social fabric of these communities. Further, improved diagnostics and disease monitoring technologies have potential to enhance foreign investment, trade, and mobility in the developing countries.[6]

Highly sensitive and specific lab assays such as cell culture methods, polymerase chain reaction (PCR), and enzyme-linked immunosorbent assay (ELISA) are available for diagnosis of infectious diseases in the developed world. They require sample transportation, manual preparation steps, and skilled and well-trained technicians. These clinical conventional methods provide results in several hours to days, precluding rapid detection and response at the primary care settings. Another diagnostic challenge is identifying multiple pathogens. Since common symptoms like sore throat and fever can be caused by multiple infectious agents (e.g., bacteria and viruses), it is important to accurately identify the responsible agent for

Received: February 1, 2013

   dx.doi.org/10.1021/cr4000623 | Chem. Rev. XXXX, XXX, XXX–XXX

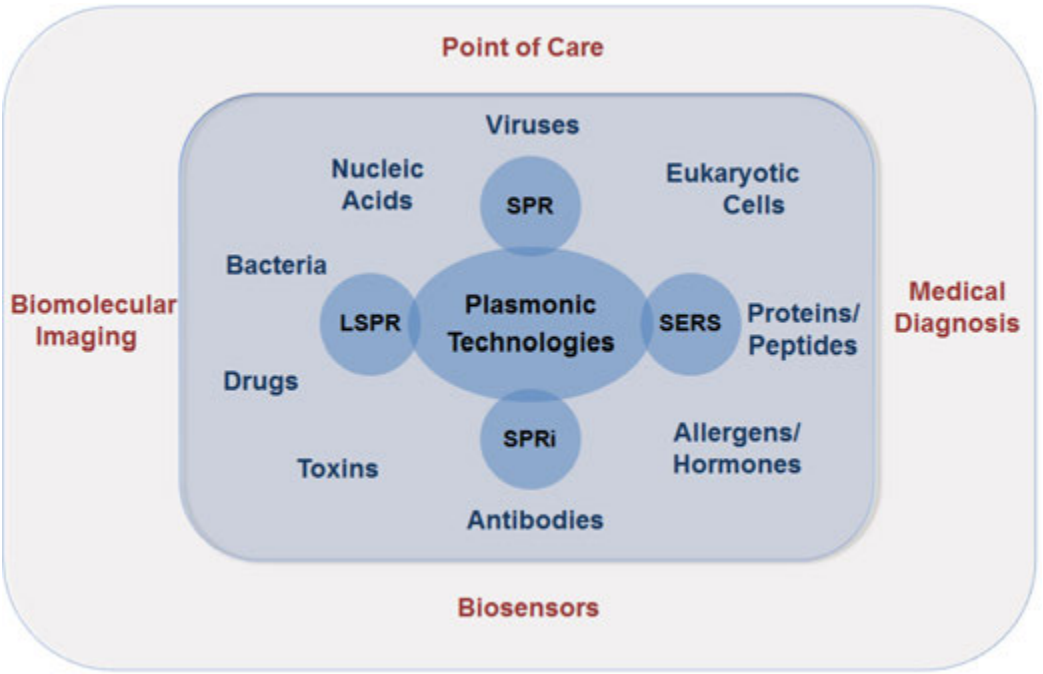

Figure 1. Plasmonic-based technologies for versatile biosensor applications. SPR stands for surface plasmon resonance, LSPR for localized surface plasmon resonance, SPRi for surface plasmon resonance imaging, and SERS for surface-enhanced Raman scattering.

targeted treatment. Therefore, high-throughput sensors for multiplexed identification would help improve patient care.[7]

Medical instruments in centrally located institutions in the developed world rely on uninterrupted electricity and running water and require controlled environmental conditions. It may not be viable to satisfy some of these criteria in some POC settings, where well-trained healthcare personnel are not available and clean water access is unreliable.[7,8] Further, in remote settings without infrastructure, rain and dust can act as contaminants.[7] Diagnostic devices for POC testing in these settings are identified by the World Health Organization to be affordable, sensitive, user-friendly, specific to biological agents, and providing rapid response to small sample volumes.[9] Optical biosensor devices are emerging as powerful biologic agent detection platforms satisfying these considerations.[10]

Optical sensing platforms employ various methods, including refractive index change monitoring, absorption, and spectroscopic-based measurements.[11] Optical sensors that are based on refractive index monitoring cover a range of technologies, including photonic crystal fibers, nano/microring resonator structures, interferometric devices, plasmonic nano/micro arrays, and surface plasmon resonance (SPR)-based platforms.[11,12] The latter two are plasmonic-based technologies. Plasmonics is an enabling optical technology with applications in disease monitoring, diagnostics, homeland security, food safety, and biological imaging applications. The plasmonic-based biosensor platforms along with the underlying technologies are illustrated in the Figure 1. Here, we reviewed SPR, localized surface plasmon resonance (LSPR), and large-scale plasmonic arrays (e.g., nanohole arrays).

The integration of plasmonics and microfluidic technologies can potentially serve the global health, primary care, and POC applications, offering modalities toward inexpensive, robust, and portable healthcare technologies. Convergence of optical technologies and microfluidic systems is promising for sensor applications by exploiting fluorescence detection, absorption, transmission, and polarization measurements on lab-chip (LOC) systems.[13] Microfluidics manipulates fluids on the microscale, minimizing the use of expensive reagents. Further, inexpensive microchip fabrication potentially allows mass production.[3a,14] Along with the capabilities of sample enrichment, isolation, mixing, and sorting, microfluidics has provided applications in several fields, including molecular biology, biotechnology, and defense.[15] These characteristics ideally position microfluidics in conjunction with plasmonic technologies to provide medical solutions at the POC and the primary care settings.

LOC devices can potentially address the challenges encountered at POC settings.[7] In these devices, single-use chips retaining the waste can be disposed of after use, avoiding contamination. The LOC system can be built from relatively inexpensive parts, specific to the disease and easy-to-operate with minimal training. The system can be designed to be portable, safe, and battery powered. Integrated microfluidic technologies with optical detection platforms such as SPR have the potential to satisfy characteristics for inexpensive, robust, and sensitive biosensors.

Here, theory and applications of plasmonic-based platforms and integration of these technologies with microfluidics are reviewed from a POC diagnostics and monitoring perspective. First, we compare the plasmonic-based biosensors with other optical, electrical, or electro-mechanical biosensor technologies. We describe the theories of SPR and LSPR and demonstrate the main experimental architecture and operational modes currently employed. We then discuss in detail the integration of microfluidic platforms, plasmonic technologies, and surface chemistry techniques leading to LOC devices. We present the current state-of-the-art plasmonic-based LOC biosensors. Finally, we provide a perspective on the future of plasmonic technologies for diagnostics and monitoring of different types of diseases, including infectious diseases and cancer, at the POC and primary care settings.

dx.doi.org/10.1021/cr4000623 | *Chem. Rev.* XXXX, XXX, XXX–XXX

Table 1. Comparison of Biosensing Technologies Considering Their Underlying Physical Mechanisms, Multiplexing Capabilities, and Limit-of-Detection Parameters

technology	physical mechanism	portability for POC	multiplexing	specificity/analyte	limit of detection	ref
SPR	optical	high	sensing and imaging	bulk solution	$(1-2.5) \times 10^{-8}$ RIU	54
			microfluidics	bacteria	$\sim 10^4-10^7$ CFUs/mL	55
LSPR	optical	high	possible to be combined with microfluidics	human immunodeficiency virus	~100 copies/mL	56
SERS	spectroscopic	moderate	possible to be combined with spri	Rhodamine 6G and Crystal Violet dyes	single molecule	26b, 57
RIfS	optical	moderate	multiwell plates	antigen−antibody interactions	19 ng/mL	58
		chemical sensing		thrombine	1.5 pg/mm^2	59
WGM	optical	moderate	polarization multiplexing	interleukin-2 (IL-2) cytokine molecule	single molecule	34
PC	optical	moderate	microfluidic integration	porcine rotavirus	36 virus focus forming units (FFU) or 0.18×10^4 FFU/mL	37
EIS	electrical	high	impedance imaging	proteins, antigens, nucleic acids, antibodies	1−10 fM	44b, 60
				human immuno-deficiency virus	10^6 copies/mL	47
AFM	electro-mechanical	moderate	simultaneous imaging and probing	ligands, streptavidin−biotin interactions	individual molecular interactions	61

2. OVERVIEW OF BIOSENSING TECHNOLOGIES

Biosensors have several crucial components: (i) a recognition element that interacts with the target; (ii) a transducer that relates the interaction of the recognition element and the target to a readable electrochemical, optical, acoustic, or piezoelectric signal; and (iii) a read-out system to interface with this signal.[16] SPR, surface-enhanced Raman scattering (SERS), whispering-gallery modes (WGM), reflectometric interference spectroscopy (RIfS), and photonic crystals (PC) provide robust and sensitive optical biosensor platforms. Micro-electro-mechanical systems (MEMs) or electrical methods also reach to low detection limits. In particular, cantilever-based sensor technologies, such as atomic force microscope (AFM), and electrical sensors, such as electrochemical impedance spectroscopy (EIS), are alternative detection techniques for biosensing applications.

SPR and LSPR technologies are based on the wave propagation or electromagnetic field enhancement phenomena near metal surfaces or nanoparticles. The propagating surface plasmon polaritons excited on plane metal surfaces are utilized in SPR sensors. LSPR relies on the field enhancement and confinement in close proximity to nanoparticles. The localized field oscillations around nanoparticles motivate the name "localized" in LSPR. The plasmon modes extend up to a couple of hundred nanometers into the biosensor medium in propagating surface plasmon polaritons (PSPP) and up to a few tens of nanometers in LSPR sensors, allowing sensitive subwavelength biosensors.[17] SPR biosensors interrogate the resonance angle changes to detect and quantify bioagents. LSPR measurements are in the form of absorbance or spectral shift data obtained from extinction curves. In general, sensitivities of these resonance or extinction shifts to refractive index changes are used to quantify figure of merit parameters for SPR and LSPR sensors.[18]

SERS is a surface spectroscopic method providing sensitive biosensor applications, and it is also a plasmonic technique, since one of the physical mechanisms behind it is LSPR.[19] In SERS, the total enhancement factor arises from (i) LSPR-enhanced Raman scattering and (ii) chemical enhancement factor.[20] Experimental biosensing demonstrations of SERS include detection of bacteria,[21] viruses,[22] DNA,[23] proteins,[24] and other small biomolecules.[25] Single molecule detection has been achieved using SERS technology.[26] The method interrogates Raman shifts originating from molecular vibrational energy levels, and therefore, allowing to distinguish structurally similar molecules if they have distinct vibrational spectra. Experimentally, the utilization of fiber optics and optofluidics, along with the use of portable spectrometers, holds potential for future label-free POC applications.[27]

RIfS, a spectroscopic method, monitors the reflected white light from thin transparent layers.[28] The reflected light from each consecutive thin layer acquires a phase shift and the resulting interference shows peaks and valleys as a function of wavelength. When bioagents attach to the surface, the constructive and destructive interference pattern of the reflected light changes. This effect can be used to monitor real-time binding events. This label-free technology has been used to detect cancer cells,[29] oligonucleotides,[30] and glycoproteins[31] and to acquire kinetic analysis of binding events.[32]

Another label-free, sensitive optical biosensor is based on the WGM technology. In this approach, tunable laser light is usually coupled to microresonators (e.g., ~100 μm diameter silica microspheres) through a fiber. Part of the incoming light is guided along the circumference of the resonator. If the light returns back in phase after every revolution, the guided wave will drive itself coherently, resulting in a resonance that can be measured as a dip in the transmission spectra. Bioagents that are in close proximity of the sensor surface cause this spectral dip to shift. This wavelength shift can be utilized in pathogen, DNA, and protein detection applications.[33] Single molecule detection is also demonstrated in modified WGM experiments.[34]

Recently, PC technology is being utilized for biosensing applications. The PCs have a photonic band gap emanating from the periodicity of the dielectric mediums.[35] Light cannot be coupled to the PCs in the band gap corresponding to a range of wavelengths. For instance, when light is incident on a one-dimensional PC, there will be a narrow spectral window with full reflection. Particles that are attached to the PC surface shift the position of this resonance band.[36] The spectral location of the band gap can be engineered by designing the

dx.doi.org/10.1021/cr4000623 | Chem. Rev. XXXX, XXX, XXX−XXX

periodicity of dielectric materials in the PC and by carefully selecting refractive indices of these materials. PC biosensors have been developed for label-free detection of bioagents including viruses,[37,38] nucleic acids,[39] proteins,[40] and cancer cells.[41]

Electrical and micro-electro-mechanical sensors provide alternatives to optical sensing methods. EIS, an electrical sensing technology, characterizes the frequency response of the impedance of a chemical system.[42] In biosensor applications, target analytes can be captured on the sensing electrode and the binding events can be recognized as capacitive changes on this electrode. Using surface modified electrodes, various EIS detection experiments have been performed, including those on cells,[43] nucleic acids,[44] bacteria,[45] proteins,[46] and DNA–analyte interactions.[42] EIS was recently used in human immunodeficiency virus (HIV) detection, where viral load is a maximum (10^6–10^8 copies/mL), through electrical sensing of viral lysate.[47] This label-free method selectively captures multiple HIV subtypes through anti-gp120 polyclonal antibodies immobilized on the surface of streptavidin-coated magnetic beads and detects the captured viruses through viral lysate impedance spectroscopy on-chip. Electro-mechanical cantilever-based technologies are primarily used for subnanometer level imaging as well as in label-free biosensing.[48] Label-free cantilever-based biosensors have been developed for detection of eukaryotic cells,[49] mRNA biomarkers,[50] protein conformations,[51] and DNA hybridization.[52] Single bacteria and single nanoparticle detection is also shown by utilizing resonators of microfluidic channels.[53]

In Table 1, we review these biosensor technologies along with the SPR technology, taking into consideration the detection limit, practicality, and multimodality parameters. Many of these technologies are close to or at the single molecule detection level, and the application needs to be evaluated when choosing the appropriate biosensor platform.

3. SPR DETECTION METHODS

3.1. Fundamental Optical Mechanisms of SPR

To analyze the propagation of surface plasmons along a metal–dielectric boundary, we consider the reflection and refraction of light between two infinite media. A linearly polarized, monochromatic light propagates from the dielectric medium toward the metallic surface, as shown in Figure 2. To explain the SPR theory, transverse magnetic (TM) polarized incident light is used. TM polarization indicates that the magnetic field vector is in the plane of the metal–dielectric interface. There is no loss of generality in using TM polarization, since transverse electric modes cannot excite surface plasmons.[62]

Solving Maxwell's equations for the p-polarized light for the wavevector components, one can find the surface plasmon dispersion relation,[63]

$$k_{1z} = \frac{\omega}{c}\sqrt{\frac{\varepsilon_1\varepsilon_2}{\varepsilon_1+\varepsilon_2}} \qquad k_{ix} = \frac{\omega}{c}\sqrt{\frac{\varepsilon_i^2}{\varepsilon_1+\varepsilon_2}} \tag{1}$$

Here, the medium is indicated by the first subscript (i.e., $i = 1$ for dielectric medium and $i = 2$ for metal medium), the axis is indicated by the second subscript, $\mathbf{k}$ is the wavevector, ω is the angular frequency of the light, c is the speed of light in vacuum, n_2 and n_1 are the refractive indices for the metal and the dielectric media, respectively, $\varepsilon_1 = n_1^2$, $\varepsilon_2 = n_2^2$, and ε_1 and ε_2 are the dielectric constants of the media. From the boundary

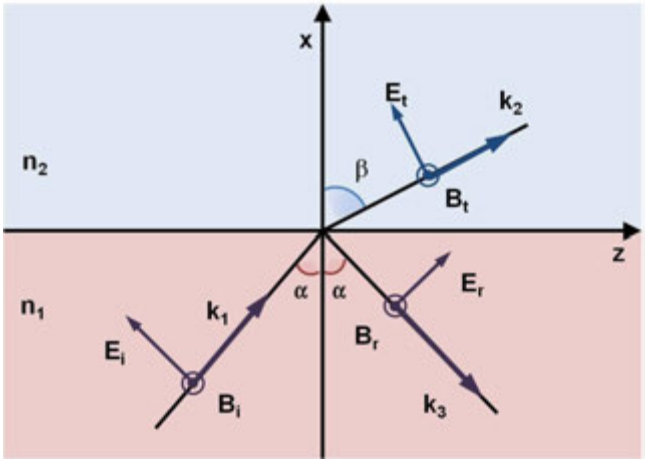

Figure 2. Plane-wave, refracting, and reflecting light at a metal–dielectric interface. n_2 and n_1 are the refractive indices of the metal and the dielectric mediums. **E** is the electric field vector, **B** is the magnetic field vector, and **k** is the wavevector. The indices i, r, and t are for incident, reflecting and refracting light. The magnetic field is perpendicular to the plane of incidence, representing transverse magnetic (p-polarized) light.

conditions it also follows that $k_{1z} = k_{2z}$. Since medium 2 is a metal, the dielectric constant ε_2 and k_{ix} are complex-valued quantities, resulting in the exponential decay of the plasmon field in both media, in the direction of the x-axis. This decay results in a surface wave, confined to the metal–dielectric interface. Physically, the incident photons couple to the free electrons on the interface, resulting in a propagating surface charge-density oscillation. The k_{1z} component of the wavevector defines the wavelength of the resonance oscillation and also the extent of the plasmon wave over the interface before absorption by the metal. For long-range and bound plasmon waves in an ideal, lossless medium, a real-valued k_{1z} and an imaginary-valued k_{ix} are required, i.e. $\varepsilon_1\varepsilon_2 < 0$ and $\varepsilon_1 + \varepsilon_2 < 0$, ignoring the imaginary parts of the dielectric constants. At optical wavelengths these two conditions are satisfied for gold and silver, which are commonly used metals in SPR experiments.[64]

Field components of the plasmon modes take their highest values at the interface and exponentially decay into the metal and dielectric media. The penetration depth of the fields into both mediums are given by $1/\mathrm{Im}(k_{1x})$ and $1/\mathrm{Im}\ (k_{2x})$, where Im is the imaginary part.[63] The penetration depth in the dielectric media is on the order of half the wavelength of the incident light. For instance, for a gold–water interface and λ = 700 nm, the penetration depth in water can be calculated to be around 238 nm.[63]

When there is a local change in the dielectric constant over the metal layer, which is caused by a molecular binding event, the surface plasmon mode energy will be changed. The SPR biosensors rely on this property of the resonance. Since the total energy of the system is conserved, the change in the plasmon mode's energy will leave a signature on the reflected or transmitted light. In SPR biosensor applications, light is monitored and analyzed to extract binding and kinetic information. This analysis is related to which method is utilized to couple the light to plasmon modes. In the following section, we overview the main light coupling methods to surface plasmon modes.

dx.doi.org/10.1021/cr4000623 | Chem. Rev. XXXX, XXX, XXX–XXX

3.2. Light Coupling Methods

To excite surface plasmons on a metal−dielectric interface, the incident light needs to provide photons that would satisfy the energy and momentum conservation laws in the light−metal system. More specifically, the incident photon's momentum and energy should match to the momentum and energy of the plasmon modes to be able to excite these charge-coupled oscillations. The preceding conditions for plasmon generation can be satisfied simultaneously only when an optical coupling element is added to the system shown in Figure 2. The common light coupling techniques utilized for this purpose are prism, grating, and waveguide coupling methods among other techniques such as waveguide, photonic crystal, and fiber-optic based coupling.[65] Physically, these modifications take advantage of attenuated total reflection (ATR), light diffraction, or evanescent wave coupling from waveguide modes in these applications.[66]

3.2.1. Prism Coupling. Otto configuration and Kretschmann configuration are the pioneering methods of prism coupling for SPR excitation.[67] In these configurations, a second dielectric layer (a prism) is added to the two-level system design considered previously, forming two interfaces. In the former case, a dielectric layer is sandwiched between a metal layer and the prism.[68] In the latter case, the metal layer is sandwiched between a prism and the sensing medium.[69]

A biosensor setup in the Kretschmann configuration is shown in Figure 3. The addition of a prism provides the necessary modification in the dispersion curves for photon-plasmon coupling. If the prism dielectric constant ε_3 is chosen such that $\varepsilon_3 > \varepsilon_1$, it is possible to satisfy the energy-momentum conservation laws for the incident light and plasmon modes, allowing for surface plasmon excitation on the metal−sensing medium interface.[70] The energy−momentum conserving equation in the Kretschmann configuration then takes the following form

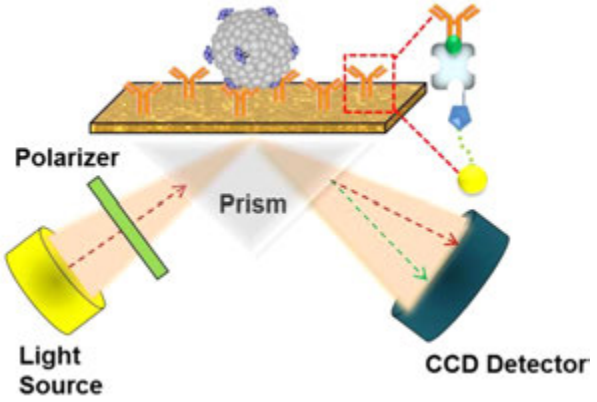

Figure 3. A biosensor design in the Kretschmann configuration is shown. The metal surface (e.g., gold) is functionalized with selective/specific recognition elements, for instance with antibodies. Transverse magnetic polarized incident light is coupled to the surface plasmon modes on the metal−sensing medium interface. The plasmon waves propagate in the immediate vicinity of the interface. When the chemically activated metal surface captures biological samples, the resulting refractive index change on the surface will modify the surface plasmon modes. These binding events will leave a signature in the reflected light, which is detected by a detector [e.g., a charge-coupled device (CCD)] for analysis.

$$\frac{\omega}{c}\sqrt{\varepsilon_3}\,\sin(\alpha) = \mathrm{Re}\{k_z\} \tag{2}$$

where k_z is the wavevector for the surface plasmon modes at the metal−sensing medium interface. Analogous equations for different coupling mechanisms are summarized in Table 2. For a given light frequency ω, the incidence angle that satisfies this equation is called the plasmon resonance angle. At this particular resonance angle, the incoming light transfers most of its energy to the plasmon modes, so the reflectivity approaches to zero at this angle.[71] The resonance angle is sensitive to small changes of the refractive index over the metal−dielectric interface. This property enables construction of biosensors that convert the shifts in the resonance angle to quantitative binding data. For instance, Figure 4A illustrates the use of a biosensor in the Kretchmann configuration with a microfluidic chip.

3.2.2. Waveguide Coupling. Waveguide structures can be used for coupling light to excite surface plasmons (Table 2). A generic waveguide coupling device model is shown in Figure 4B. The propagating wave intensity in the waveguide is concentrated in the planar waveguide structure, while a small portion of the light extends through the metal layer to the metal−sensing medium interface and induces surface plasmons. This phenomenon is realized in a narrow wavelength range (resonance wavelength) and presents itself in the transmitted light spectra.[72] Therefore, the wavelength spectra at the output port of the waveguide can be monitored for biosensing applications. The shift of the resonance wavelength will allow quantification of the captured agents.[73] Fiber-optic-based coupling approach provides a special case of this method that the fiber-optic cables are cylindrical optical waveguides working with total internal reflection principle. Figure 4C shows a generic fiber-coupled SPR device. The propagating light bounces from the higher refractive index cladding while propagating in the lower refractive index core of the fiber. A portion of the cladding can be removed and coated with a thin metal layer which is in contact with the sensing layer. The incident light on the metal layer reaches to the metal−sensing layer interface as an evanescent wave and induces surface plasmons on this interface.[74]

3.2.3. Diffraction Grating Coupling. Two dimensional metallic gratings can be used to couple light to plasmon modes on interfaces. Figure 4D illustrates a grating coupled biosensor operating in the transmission mode. The momentum-matching condition becomes a function of the grating order m, an integer value related to the diffracted light direction (Table 2). Transmitted or reflected light from grating coupled plasmonic biosensors can be studied under intensity, wavelength, or angular interrogation.[75]

3.2.4. Photonic-Crystal-Based Coupling. In recent years, new coupling methods have also been attracting attention. Various PC-based sensors were realized with planar-waveguide fibers, microstructured PC fibers, and PC Bragg fibers.[76] In the planar-waveguide structure, the core is covered with a periodic PC structure (Figure 4E). One side of the waveguide is gold coated and is in contact with the analyte for plasmonic detection. The microstructured PCs are being explored in several design alternatives.[77] In general, the fiber is made of silica glass.[78] The air-filled geometric holes provide the periodic structure for the photonic crystal (Figure 4F). The semicircular shapes are analyte filled microchannels. These channels are gold-coated for surface plasmon excitation and detection. These

dx.doi.org/10.1021/cr4000623 | Chem. Rev. XXXX, XXX, XXX−XXX

Table 2. SPR Coupling Methods and Coupling Equations

coupling method	coupling equation[a]	equation parameters
prism coupling (Kretschmann configuration)	$\frac{\omega}{c}\sqrt{\varepsilon_3}\sin(\alpha) = \mathrm{Re}\{k_z\}$	ε_3 is the dielectric constant of the prism, c is the speed of light, ω is the angular frequency of the light, and α is the incidence angle
waveguide coupling	$\beta_{\mathrm{waveguide}} = \mathrm{Re}\{k_z\}$	$\beta_{\mathrm{waveguide}}$ is the propagation constant for the waveguide mode.
grating coupling	$m\frac{2\pi}{\Lambda} + k_0 = \pm\mathrm{Re}\{k_z\}$	Λ is the grating period, k_0 is the component of the incident light parallel to the interface, and m is the grating order.

[a] k_z is the wavevector for the surface plasmon modes at the metal-sensing medium interface. Re{} indicates the real part of the argument.

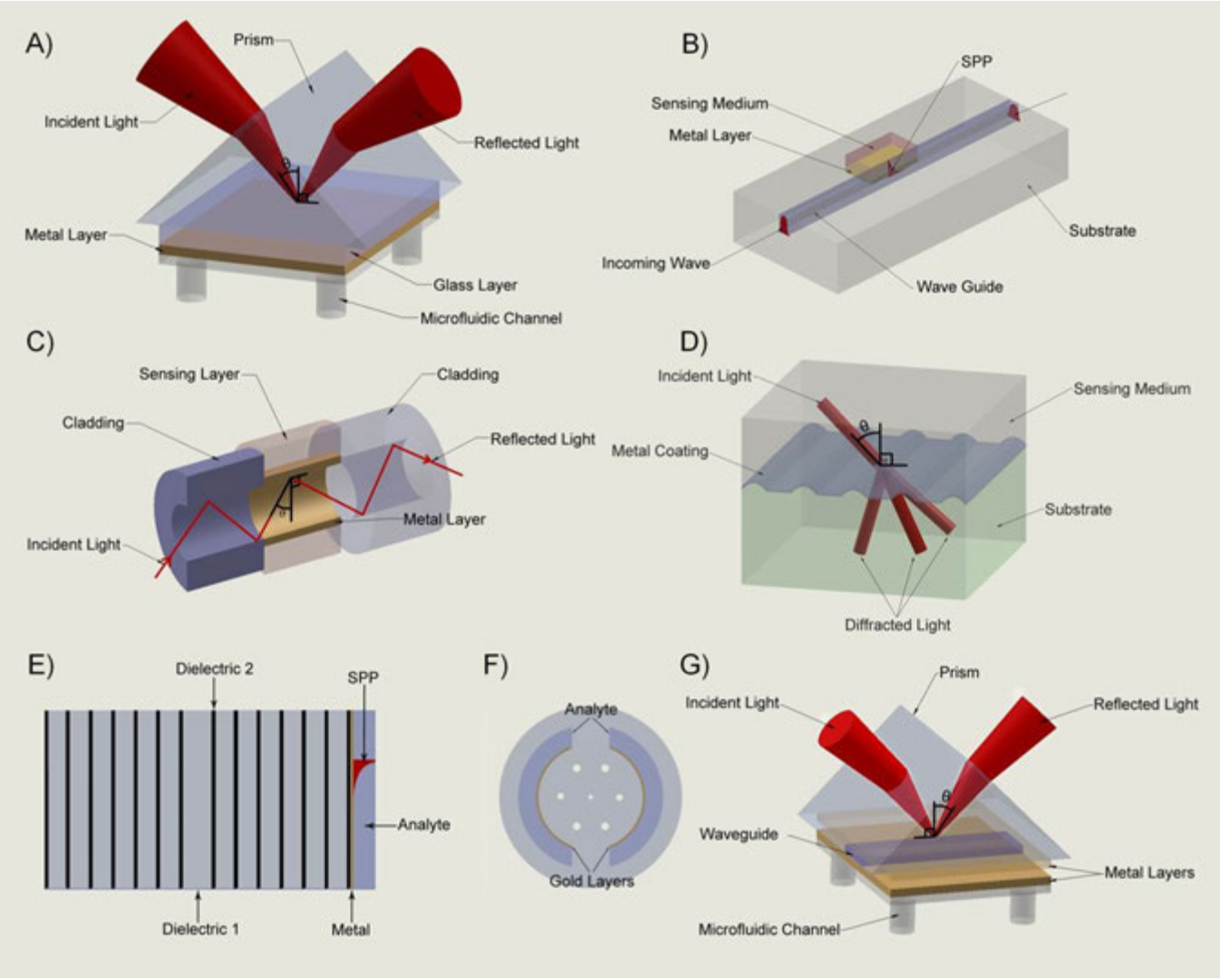

Figure 4. Most common surface plasmon operation modes for light coupling: (A) Kretschmann configuration for prism coupling, (B) waveguide coupling, (C) fiber-optic based coupling, (D) grating coupling, (E) planar waveguide photonic crystal coupling, (F) honeycomb photonic crystal coupling, (G) waveguide-based coupling in Kretchmann configuration.

technologies can be used with microfluidics to provide integrated biosensors.

3.2.5. Combined Coupling Methods. A number of the preceding methods have been proposed to be used together for plasmonic biosensor architectures. One example is provided by the prism-coupled waveguide plasmon excitation scheme.[79] In this method a polymer waveguide is sandwiched between two metal layers (Figure 4G). A prism is used to couple the incident light to plasmon modes on one of the metal layers. The polymer waveguide can be electro-optically modulated to a desired refractive index. This tuning of the waveguide-coupled surface plasmon modes makes sensitive surface plasmon angle interrogation possible by utilizing modulation and demodulation techniques.

3.3. Localized Surface Plasmon Resonance

LSPR sensing is a spectroscopic technique based on the strong electromagnetic response of metal nanoparticles to refractive index changes in their immediate vicinity. When light is incident on nanoparticles, particular electronic modes can be excited so that the conduction band electrons oscillate collectively.[80] As a result of these resonance oscillations, also

dx.doi.org/10.1021/cr4000623 | Chem. Rev. XXXX, XXX, XXX–XXX

called localized surface plasmons, the nanoparticles strongly scatter light at a specific wavelength range. The plasmon oscillations obtained by solving Maxwell's equations around metal nanoparticles are illustrated in Figure 5.[81] The sum of

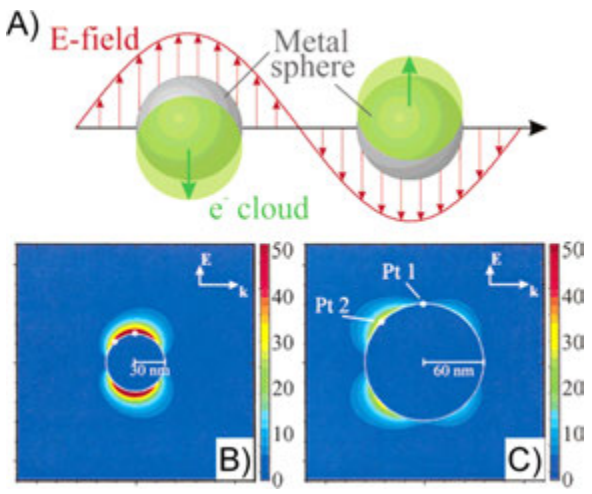

Figure 5. Electric fields around nanoplasmonic silver particles. (A) Illustration of the plasmon oscillation and the electron cloud on metal spheres. (B) Electric field contours of the main extinction peak 30 nm silver spheres in vacuum. Cross section of the sphere is shown with 369 nm light. (C) Electric field contours on 60 nm radius silver spheres in a vacuum. A cross section of the sphere is shown with 358 nm light and the field is from the quadropole peak. Adapted with permission from ref 81. Copyright 2003 American Chemical Society.

light scattering and absorption is called extinction, and it is possible to observe the optical response of individual nanoparticles using dark-field microscopy.[82] In biosensing applications, the attachment of an analyte to these nanoparticles results in a refractive index change, causing a red or blue shift in the extinction peak wavelength, λ_{max}. This shift in λ_{max} is given by the following equation[83]

$$\Delta\lambda_{max} \cong m\Delta n[1 - \exp(-2d/l_d)] \quad (3)$$

where m is the sensitivity factor, Δn is the change in the refractive index, d is the effective adsorbate layer thickness, and l_d is the electromagnetic field decay length. The extinction is maximized by optimizing the nanoparticle characteristics described by m and l_d, and it is already well-established that the extinction is a strong function of the nanometal's type, size, shape, and orientation.[84] Exploitation and design of these parameters will be essential for new effective LSPR applications.[84]

LSPR sensing experiments utilize a white light source covering the visible spectrum.[85] The scattered light is collected with a spectrometer, and changes in the spectra are then converted to binding data.[80] In these experiments, light is directly coupled to the sample without requiring a prism or a grating, as in the SPR technique; therefore, the angle of incidence does not need to be precisely controlled. In contrast to the SPR technique, LSPR sensors based on nanoparticle surfaces are less sensitive to thermal variations.[18a,65,86] In addition, with the availability of portable spectrometers, it is likely that LSPR applications can be translated for portable diagnostic applications.

3.4. Nanoplasmonic Arrays

Array-based nanoplasmonic detection is a plasmonic technique, similar to SPR imaging (SPRi) in the sense that it can be used for high-throughput biosensing applications. Various nanoplasmonic arrays have been demonstrated for refractive-index-based sensors, including nanoholes,[87] nanowells,[88] nanoposts,[89] nanopillars,[90] nanorods,[91] nanodisks,[92] nanotubes,[93] and nanopyramids.[94] These periodic arrays present high reproducibility in sensor fabrication, allow spectroscopic and intensity based measurements, and have a small footprint. A number of fabrication techniques are used for large-scale arrays, including focused ion beam milling and soft lithography techniques.[95] However, they require expensive fabrication methods that are not suitable to create inexpensive devices.

Nanohole arrays are usually made from perforated metal films supported on substrates such as silicon nitrides. These arrays are based on the extraordinary optical transmission (EOT) effect[96] and find applications as refractometric

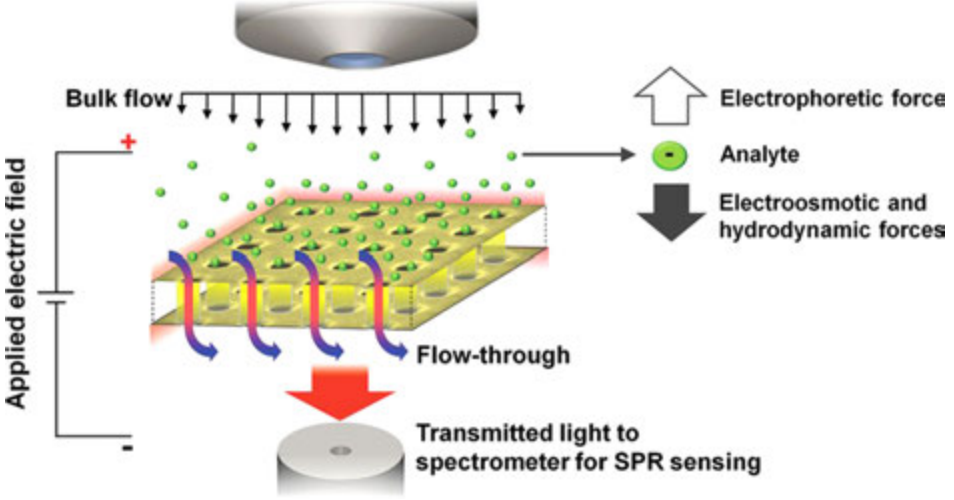

Figure 6. A nanohole array integrated with fluidics. The flow-through plasmonic nanostructure enabled local concentration of analytes. The method presented 100-fold concentration and simultaneous sensing of a protein. Further, the method presented 10-fold improvement in sensing speed in comparison to the control experiment with no analyte concentration. Reprinted with permission from ref 101a. Copyright 2012 American Chemical Society.

dx.doi.org/10.1021/cr4000623 | *Chem. Rev.* XXXX, XXX, XXX–XXX

sensors.[97] In nanohole arrays, localized and propagating SPR modes are intercoupled.[98] The resulting resonance modes are influenced by the periodicity, size, and shape of holes in the array and the composition of materials used in the sensor.[97a,99] Extensive numerical calculations have been used to gain insight for the optimization of these parameters.[100] These periodic arrays can be used in the flow-through geometry in biosensors, which enables concentrating analytes under applied electric fields (Figure 6).[101] This operation mode lets analytes pass through the nanochannels, which are also forming the plasmonic structure of the sensor, and was shown to improve mass transport properties and response time.[87]

From a POC perspective, combination of array-based sensors with microfluidic chips can allow high-throughput sensors. Since each array can be interrogated separately and multiple arrays on parallel microchannels can be fabricated, nanohole array sensors are suitable for multiplexed on-chip detection. Light can be coupled directly to the sensor at or close to normal incidence, and the transmitted light can be interrogated with a CCD sensor.[102] The imaging mode permits use of high numerical aperture optics, allowing wide-field imaging from densely packed arrays.[103] Microfluidic integrated nanohole arrays have been used for analyzing antibody–ligand binding kinetics[104] and biomarkers.[101b] A recent application of nanoholes incorporated 50 microfluidic channels (30 μm width, over a 3.5 × 2 mm area) and utilized high-throughput SPR imaging.[105] The system was used for real-time affinity measurements.

Capture of intact viruses has been earlier shown from unprocessed whole blood on microchips.[106] Nanoholes have potential to be used in optofluidic biosensor applications, as recently demonstrated in the detection of pseudoviruses (i.e., pseudotyped Ebola virus) and intact Vaccinia virus at 10^8 pfu/mL in PBS.[107] However, this platform needs to be expanded to detect viruses from bodily fluids at clinically relevant concentrations for diagnostic applications.

4. INTEGRATION OF PLASMONIC TECHNOLOGIES WITH MICROFLUIDICS

The integration of microfluidics and plasmonics brings the capability to build label-free and reliable biosensors on a LOC platform. Microfluidics has been widely used in cell separation and isolation and preparation, analysis, and delivery of samples.[85,108] In particular, microfluidic technologies for blood cell separation and plasma isolation are significant for clinical applications.[109] Integrated microfluidic devices with various fluid manipulators including pumps, mixing systems, separators, and valves have already been demonstrated.[110] Complete processing and analysis of various bioagents have been shown on LOC microfluidic devices.[111] For instance, DNA purification from bacteria on a single microfluidic chip has been shown without either pre- or post-sample processing.[112]

Combining microfluidics with optics provides a rapidly expanding range of applications by bringing advantages from these fields. Microfluidic-based plasmonic devices are refractive index monitoring type devices. This class of devices can be considered as a subtype of optofluidics devices. On one hand, light can be used to direct the motion of fluids in microfluidic chips. Optical-tweezers-based approaches have been used to build valves and pumps to induce flow in microfluidic channels.[113] Blood cell separation has been demonstrated by utilizing optical lattices.[114] On the other hand, fluids can be used to alter optical parameters, as in plasmonics. Refractive index, absorption, polarization, and spectral properties can be monitored for various plasmonic biosensor designs. A further advantage of plasmonics is to allow label-free signal transduction method.

The two main optical biosensor design considerations are light–analyte interaction volume and sample delivery, which can seriously constrain the use of biosensors. The former consideration can be addressed by plasmonics taking advantage of the evanescent electromagnetic fields. For instance, the evanescent fields generated by the surface plasmon polaritons in SPR extend a few hundred nanometers into the fluid and allow low analyte densities to be detected. The latter consideration can be addressed by microfluidics, which can manipulate microliter quantities of fluids.[115] Further, selective delivery of analytes through multiple channels can be engineered for high-throughput microfluidic applications.

In plasmonic-based LOC biosensors, a recognition element is immobilized on the detection surface for label-free sensing. The choice of the recognition element depends on a number of factors, including the specificity and affinity toward the target molecule. Further, the complex formation between the recognition element and the target molecules should be stable in structure. Various surface functionalization techniques exist for the immobilization of these moieties for stable, high-density and efficient binding. We review these techniques in the following section.

4.1. Surface Functionalization

Biosensing platforms are comprised of a sensing support surface (e.g., gold and silver) and an immobilized biomolecular recognition element (e.g., antibodies, oligonucleic acids, peptide nucleic acids, peptides, and polymers).[116] The support surface enables the recognition element to be stable and allows them to interact with the target analytes. Depending on the sensitivity, specificity, and limit of detection, the recognition element is immobilized through several surface techniques, including physical adsorption, chemical adsorption, covalent binding, and affinity-based interactions.[116a] Besides these common methods, recent advances in surface functionalization and antifouling agents to minimize nonspecific binding are also reviewed in the following subsections.

4.1.1. Physical Adsorption. Physical adsorption technique utilizes the surface characteristics and surface charge to attach and immobilize biorecognition elements onto the surface and relies on nonspecific physical interactions between the recognition element and the support material.[117] In contrast to chemical binding techniques, this method also holds a key advantage since it does not require any reagent to activate chemical groups on the surface, and thus, this technique is easy to perform, inexpensive, and reduces structural damage in biorecognition elements. The physical adsorption method particularly utilizes hydrogen bonding and van der Waals forces.[118] These weak interactions also allow the biorecognition elements to easily detach from the surface, and thus, the biosensing surface can be used multiple times. However, nonspecific physical interactions are closely affected by environmental changes, including temperature, ionic content, and pH. On the other hand, this technique causes nonspecific binding of other molecules and substances, resulting in a significant decrease in surface coverage of the recognition elements and sensor specificity.

The support materials can be modified to generate surface charge and reactive groups using oxidizing techniques such as oxygen plasma treatment. Oxygen-plasma-treated and untreated polystyrene (PS) slides have been recently used as sensor substrates to detect breast cancer type 1 (BRCA1) gene mutations, and these two cases were compared in terms of uniform immobilization and binding capacity of a biorecognition element (i.e., oligonucleotide−protein conjugate).[119] On plasma-treated slides, the binding amount of oligonucleotide−protein conjugates significantly increased compared to untreated slides.[119] Another interesting observation in this study was that plasma treatment amplified the surface area and formed nanoroughened structures that could facilitate detection of a low amount of target analyte and improve the analytical performance of the biosensing surface in microarray applications.[119] Although oxygen plasma treatment is a simple and effective method for many surfaces, it often causes significant damage on the biosensing support surface.[120] This major obstacle leads to permanent surface disruptions, which interfere with the sensor surface structure and reduce sensitivity.[120] On the other hand, the surface characteristics (e.g., hydrophobicity and polarity) and the functional groups of biomolecules determine the molecular interactions for biomolecule immobilization. Although, in some cases, the orientation of the recognition element is not critical to capture the target analyte, these molecular changes on the surface can affect biomolecular activity (e.g., denaturation of proteins) and orientation of proteins and antibodies due to the restrictions in their conformational flexibility.[121]

4.1.2. Chemical Adsorption and Covalent Binding. Chemical adsorption and covalent binding techniques are most frequently combined to form chemical coupling and bond formation between support surface and biorecognition elements in three main steps: (i) support surface activation, (ii) functional group generation, and (iii) biomolecule immobilization.[116a] The self-assembled monolayer (SAM) technique, one of the most common chemical adsorption techniques (i.e., chemisorption), spontaneously generates self-formation of molecular assemblies on substrates.[122] *N*-alkylthiols or disulfides are the most common SAM molecules, consisting of an alkyl backbone chain, thiol head, and functional tail groups.[116a,123] On these molecules, thiol head groups have strong affinity to bind to metal surfaces (e.g., gold and silver), and the alkyl backbone tethers the biomolecules from the substrate. The latter group presents a functional end to interact and covalently bind to biomolecules.[116a] Coupling reactions (e.g., *N*-hydroxysuccinimide (NHS) and ethyl-(dimethylaminopropyl)carbodiimide (EDC)) are the most common biomolecule immobilization methods that typically form succinimide groups that interact with amine groups of organic molecules (e.g., antibody, protein, nucleic acids, and amine-modified lipids).[124] By utilizing covalent bonding, modified SAM agents (e.g., 11-mercaptoundecylamine (MUAM) and dithiobis(*N*-succinimidyl propionate) (DTSP)) were previously used to immobilize double-stranded DNA, peptide nucleic acid (PNA), and miRNA on SPR gold sensors for the detection of nucleic acids.[125] Other than the SAM mechanism, biomolecules can be immobilized through silanization agents (e.g., (3-aminopropyl)triethoxysilane (APTES) and (3-aminopropyl)trimethoxysilane−tetramethoxysilane (MPTMS or 3-MPS)) that cover a biosensing surface (e.g., glass, mica, metal oxides, and silica) with functional alkoxysilane molecules by forming a covalent Si−O−Si bond.[108c,126] This process can also be coupled with another reaction as performed in SAM modifications.[108c,121,127] On the same platform, long- and short-chained SAMs can also be utilized to block the surface from nonspecific binding.[128] Further, long-chained SAMs can be used to construct artificial lipid bilayer systems using hydrophobic interactions between alkyl backbones and lipid tails.[129] For instance, artificial lipid bilayers are constructed by the rupture of liposomes, and self-assembled hexadecane monolayer surface assists to rupture liposomes for the formation of lipid bilayers on gold surfaces.[129] Thus, self-assembled hexadecane monolayer surface provides a dynamic and stable structure to tether lipid bilayer and allows for further biomolecular analyses such as polymer−lipid bilayer interaction in vitro conditions.[129] Additionally, SAMs can be used to immobilize protein conjugate, oligonucleic acids, and peptide nucleic acids for microarray analysis.[130] However, there are some limitations in SAM formation, including availability of substrate, low number of organic molecules for monolayer formation, the choice of anchoring groups, and limited solubility of monolayer molecules.[122] Additionally, bulky monolayer molecules result in large defects in monolayer structure and lack of thermal and oxidative stability restricting their large-scale use in detection platforms.[122]

4.1.3. Affinity-Based Interactions. Affinity-based surface functionalization techniques address some of the current challenges in biomolecule immobilization methods mentioned above. Avidin−biotin-based interactions are commonly used to immobilize biomolecules (e.g., nucleic acids, proteins, and antibodies) on the biosensing surface without interfering with their biomolecular structure and function.[106b] For instance, NeutrAvidin and streptavidin are well-known members of avidin proteins, and they have high association capacity to biotinylated molecules such as antibodies, nucleic acids, peptides, and PNA. An interesting example for biotin−avidin-based surface functionalization is traptavidin, which is an engineered mutant version of streptavidin protein according to biotin−4-fluorescein dissociation rate.[131] This mutant avidin protein has lower flexibility in the biotin-binding pocket, and this structural property reduces the entropic energy required for biotin binding.[131] Thus, traptavidin structurally inhibits the dissociation rate and enhances thermostability compared to native avidin proteins. Traptavidin is also a versatile protein that can bind to a range of biotin conjugates (i.e., biotin−4-fluorescein, biotin−amidocaproyl-BSA and biotinylated DNA (internal and terminal)).[131] Therefore, this protein holds a great potential to replace other avidin-based proteins in nanoplasmonic detection platforms, molecular anchored arrays, and POC diagnostic technology platforms.[131] However, the biotinylation site is a critical parameter for biomolecule (e.g., antibody) orientation in avidin−biotin-based surface chemistries. Two groups of affinity-based surface chemistries (i.e., protein G- and NeutrAvidin-based) were evaluated, and the observations obtained from AFM demonstrate that protein G-based surface chemistry can efficiently immobilize the antibodies with their favorable orientation in microfluidic channels.[106b] Since protein G has a specific binding site for the fragment crystallizable region (Fc) of antibodies, it provides better control over antibody orientation.[106b] To increase the number of antibody binding sites and stability, immunoglobin specific proteins are engineered using recombinant DNA technology. Protein A/G is a notable example of the recombinant antibody immobilization molecules that combines IgG binding domains of both protein A and protein G. This recombinant fusion

dx.doi.org/10.1021/cr4000623 | *Chem. Rev.* XXXX, XXX, XXX−XXX

protein is comprised of four Fc binding domains from protein A and two from protein G, and it is more stable to pH changes compared to protein A.[107,132] Overall, affinity-based surface functionalization methods increase sensitivity and capture efficiency and improve the detection limit to capture target molecules/bioagents by utilizing high binding affinity and controlling molecular orientation. Additionally, oligonucleotide immobilization for nucleic acid hybridization studies and histidine-chelated metal ion methods for protein-based detection are widely used in the immobilization of biorecognition elements.[133] There are also new surface functionalization methods, including polymeric coating, lipid bilayer construction, PNA, and aptamer immobilization, to capture target analytes in POC and primary care diagnostics for various applications ranging from early cancer detection diagnosis and monitoring of infectious diseases.

4.2. Blocking of Nonspecific Binding

Nonspecific binding to biosensing surfaces is one of the major drawbacks for specific capture and quantitative analysis.[134] One of the challenges is the concentration of other substances being higher than target analyte since these substances can also bind/attach to the biosensing area.[135] Although the binding characteristics of nonspecific interactions is much different than that for a specific binding event, nonspecific interactions and binding still poses a significant bottleneck for limit-of-detection in biosensors. Further, nonspecific binding can occur at functionalized, passivated, and untreated regions of the biosensing area.[135] Thus, these nonspecific interactions can decrease detection sensitivity. There are several antifouling agents (e.g., chemical, protein based, and polymeric agents) used to address these challenges by improving the specificity.

Thiol compounds have been commonly used as chemical blocking agents on metal surfaces. The length and terminal group of thiol compounds affect the sensitivity and detection limit.[136] To evaluate these parameters, a number of alkanethiol SAMs (i.e., 3-mercapto-1-propanol (3-MPL), 6-mercapto-1-hexanol (6-MHL), 8-mercapto-1-octanol (8-MOL), 9-mercapto-1-nonanol (9-MNL), 11-mercapto-1-undecanol (11-MUL) and another blocking thiol (C_{11}) with a $-CH_3$ terminating headgroup, and 1-dodecanethiol (1-DDT)) was used for the detection of the target DNA sequences using pyrrolidinyl peptide nucleotide acid (acpcPNA) probes that were immobilized via a spacer molecule.[136] The blocking thiol compound with same length (9-MNL) as the total spacer molecule provided the highest sensitivity [20.4 ± 0.7 nF cm^{-2} (log M)$^{-1}$] compared to the other thiol blocking agents with shorter and longer length.[136] This specific length possibly arranged more favorable hybridization, resulting in the highest hybridization efficiency, whereas the blocking agent with longer length overlapped with the probe.[136] The terminal groups (i.e., $-OH$ and $-CH_3$) of thiol blocking agents were also evaluated on the same platform, and the hydroxyl-terminated agent provided a slightly better sensitivity by increasing hydrophilicity for DNA immobilization and hybridization.[136] Proteins (e.g., bovine serum albumin, casein, glycine, and gelatin) have been also used to protect the biosensing surface from nonspecific interactions. Instantized dry milk, casein, gelatins from pig and fish skin, and serum albumin were evaluated to understand the blocking capabilities, and casein and instantized milk were observed to inhibit nonspecific binding.[137] In this study, porcine skin gelatin was observed to be the least effective antifouling agent.[137] Overall, the critical parameter for protein blocking experiments is that blocking agent (e.g., casein) primarily interacts with the biosensing area instead of blocking the protein−protein interactions observed in porcine skin gelatin experiments.[137] However, the efficiency of these natural blocking agents (e.g., albumin, casein, and glycine) is not considerably satisfactory.[138] In contrast, polymeric blocking agents are easily reproducible and can be modified to increase the specificity of blocking.[138] Polyethylene glycol (PEG) is one of the most common polymeric blocking agents, and a densely packed PEG tethered-chain surface allows one to minimize nonspecific binding.[138,139] The combination of long and short PEG chains significantly reduces biofouling on the biosensing surface and increases the sensitivity.[138,140] Factor IX (FIX) was immobilized on glutaraldehyde-activated surface and detected via its aptamer.[138] A copolymer (i.e., poly(ethylene glycol)-*b*-poly(acrylic acid) (PEG-*b*-PAAc)) was used as a blocking agent to reduce nonspecific binding on untreated and glutaraldehyde-activated regions.[138] The limit of detection was observed to be down to 100 pM.[138] The sensitivity was further improved by using dual polymers (i.e., PEG-*b*-PAAc and pentaethylenehexamine-terminated PEG (N6-PEG)) on the same platform, and 1000-fold better sensitivity (100 fM) was achieved with respect to the blocking with PEG-*b*-PAAc.[138] Here, the use of dual polymers demonstrates higher sensitivity and reliability for the biosensing platforms that detect a very small amount of target molecules from complex fluids such as whole blood.[138] Apart from these surface modifications, the generation of nanorough surfaces allows one to prevent the bacterial attachment on biosensing surface.[141]

4.3. Recent Advances in Surface Functionalization

Within the past decade, conventional surface functionalization methods have been replaced with new surface modification materials (e.g., lipids and polymers) and techniques (e.g., thiol exchange and site-specific functionalization). These innovations improve the molecular interactions between target molecule and the receptor of interest, and they enable more stable structures for biosensing platforms.[142] For instance, receptors (e.g., integral proteins) incorporated with cellular membranes require hydrophobic content to conserve their native structure and function in biosensing platforms.[142c] Dynamic, flexible, and complex nature of the cellular membranes is an attractive candidate to support biorecognition elements such as receptors for these platforms.[142c] Noncovalent assembly of lipid bilayers on biosensing surfaces combines highly sophisticated surface modification mechanisms with a nature-synthesized functional platform.[142c] The arrangements of lipid bilayers also allow one to monitor membrane-associated molecular recognition events on the close vicinity of the membrane using surface sensitive tools such as LSPR and SPR.[142c] To construct lipid bilayers on biosensing platforms, specific surface immobilization strategies are employed using tethering agents that rupture lipid vesicles to form a planar lipid bilayer.[142b,143] This strategy can be done by utilizing a thin layer of SiO_2 on plasmonic substrate.[144] Other construction strategies are the use of thiolated lipids that covalently immobilize lipid membrane to metal substrate and utilization of a polymer cushion that tethers lipid membrane and forms an ionic reservoir for functional integration of receptors.[145]

Chemical modification and physical properties of lipid molecules have allowed lipid bilayers to be used in surface sensitive biosensing approaches, including the detection of biomolecules, proteins, and nucleic acids. Biotinylated-lipid

dx.doi.org/10.1021/cr4000623 | Chem. Rev. XXXX, XXX, XXX−XXX

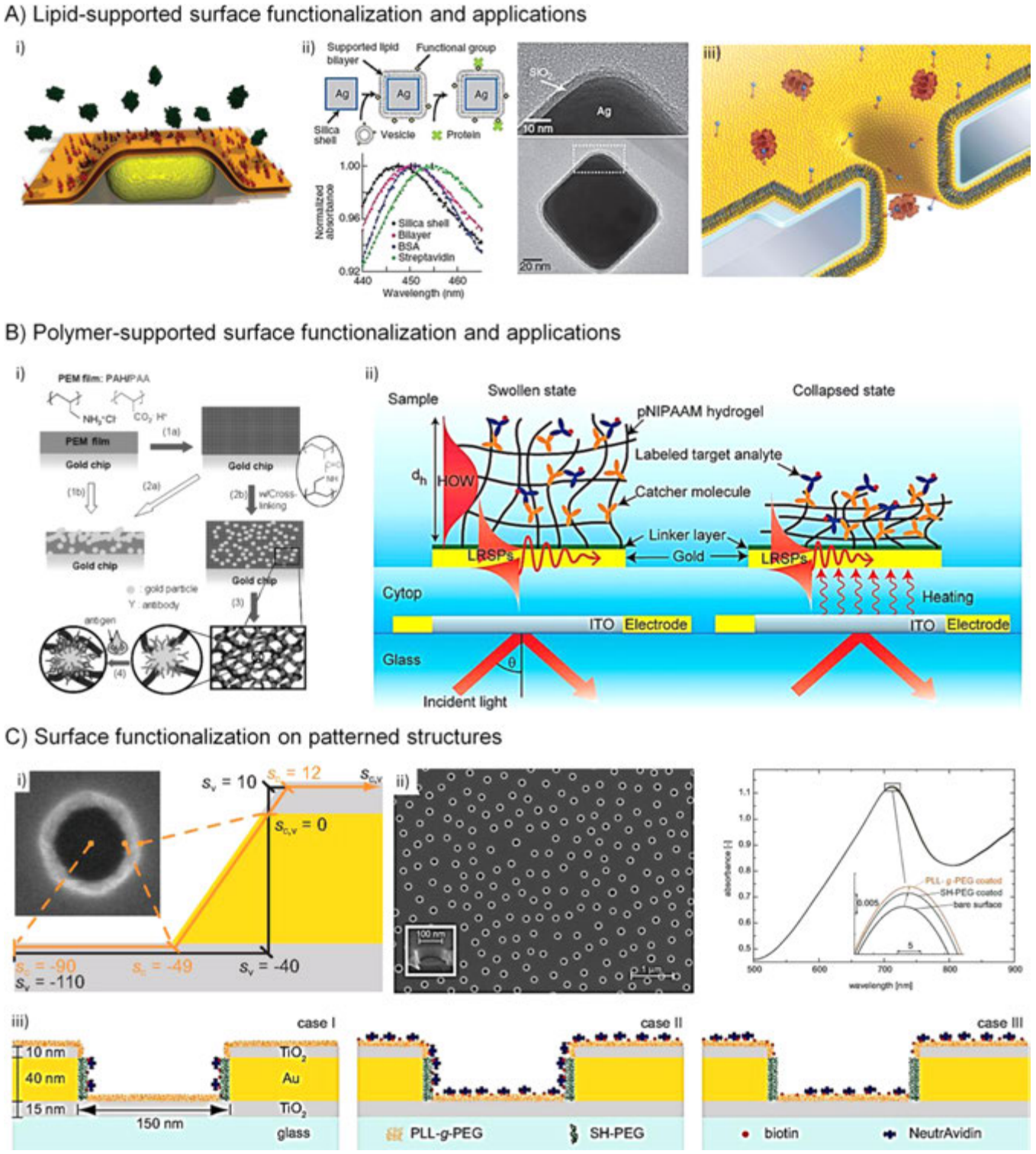

Figure 7. Recent advances in surface functionalization methods and materials. (A) Lipid-supported surface functionalization and applications: (i) Schematic of a gold nanorod coated with a biotinylated lipid membrane and interactions with streptavidin. Adapted with permission from ref 146. Copyright 2008 American Chemical Society. (ii) Schematic of supported lipid-bilayer-coated core shell nanocubes (Ag@SiO_2). TEM images of whole and select region of a Ag@SiO_2 nanocube. A solution-phase plasmonic sensor measures LSPR spectra of surface modification and coating on Ag@SiO_2 core shell nanocubes using a standard laboratory spectroscopy. Adapted with permission from ref 147. Copyright 2012 Nature Publishing Group. (iii) Schematic of lipid-bilayer-coated nanopore in silicon nitride substrate. This platform facilitates mobility of target molecules and minimizes clogging. Adapted with permission from ref 150. Copyright 2011 Nature Publishing Group. (B) Lipid-supported surface functionalization and applications: (i) The procedure of a gold-nanoparticle-hybridized polymer film for biosensing applications. Adapted with permission from ref 151. Copyright 2009 Wiley-VCH Verlag GmbH & Co. KGaA. (ii) SPR-based biosensing platform with embedded indium tin oxide microheater and rapid tuning of SPR signal using a thermoresponsive polymer (i.e., pNIPAAm). Reprinted with permission from ref 152. Copyright 2013 American Chemical Society. (C) Surface functionalization on patterned surfaces: (i) Schematic and scanning electron microscopy (SEM) image of the patterned nanostructures (i.e., nanoholes). (ii) SEM top-view image of nanholes and extinction peak values of LSPR spectra for surface

dx.doi.org/10.1021/cr4000623 | *Chem. Rev.* XXXX, XXX, XXX–XXX

Figure 7. continued

modifications. (iii) Nanoholes arrays consisting of TiO_2/Au/TiO_2 films are specifically modified with poly-L-lysine−poly(ethylene glycol) (PLL−PEG) and thiolated PEG (HS-PEG) molecules for site-specific surface functionalization. Adapted with permission from ref 158. Copyright 2010 American Chemical Society.

membranes were immobilized to detect streptavidin molecules on the surface of gold nanorods by monitoring the spectral shifts using a fast single particle spectroscopy (fastSPS) instrument coupled with dark-field microscopy (Figure 7A-A(i)).[146] The binding of streptavidin molecules to a single nanorod resulted in a median shift of 2.9 ± 1.8 nm when 29 nanorods were analyzed.[146] Thus, on this platform, local interactions of proteins with cellular membranes could be monitored in real-time.[146] Another interesting example was to assess the binding of target proteins to supported lipid-membrane-coated nanocubes (Figure 7A(ii)).[147] Here, the researchers reported a solution-phase plasmonic sensor method that utilizes LSPR spectra of Ag@SiO_2 core shell nanocubes using spectroscopic measurements (Figure 7A(ii)).[147] In this work, supported lipid bilayers were spontaneously formed by mixing Ag@SiO_2 core shell nanocubes in lipid-vesicle solution, and the plasmonic response of the platform was calibrated by examining the binding of streptavidin to biotinylated lipid molecules in the supported membrane. LSPR response was then converted to protein coverage on the nanocube surface by utilizing the LSPR shifts to protein mass change, and the limit of detection was reported as 0.191 ng/mm^2 nm.[147] Further, cellular-membrane-associated molecular interactions were assessed on the supported lipid-bilayer-modified gold nanoparticles using a single nanoparticle tracking-based detection method.[148] The binding and molecular interactions of membrane-associated molecules (i.e., cholera toxin B subunit and ganglioside GM1 pentasaccharide head-groups) were evaluated using the diffusion coefficients of gold nanoparticles on the membrane.[148] The limit of detection for the cholera toxin B subunit was observed to be down to 10 pM, resulting in 100-fold improvement in the sensitivity compared to fluorophore-based methods.[148] Thus, an ultrasensitive detection platform was developed by utilizing the mobility of lipid molecules in membranes.[148] Additionally, supported lipid membranes were employed on nanopore assays for the detection of small molecules (e.g., proteins) and the monitoring of DNA hybridization and receptor−target interactions.[142c,149] The integration of lipid bilayers with nanohole platforms facilitated more frequent translocation/mobility of target molecules and, thus, introduced chemical sensitivity and avoided clogging, which are major obstacles in biosensing assays (Figure 7A(iii)).[142c,150] Overall, lipid-bilayer-incorporated biosensing platforms improve the molecular interactions and form a support layer for the integration of biorecognition elements. Thus, this new surface functionalization strategy can be used for membrane-associated molecule biosensors and toxin/drug screening assays in the future.

Polymer-mediated surface functionalization is another interesting strategy to generate a support layer for the immobilization of biorecognition elements. Polymers play a vital role to enhance the reliability and sensitivity of biosensors, and they are often used for hybridization with plasmonic nanoparticles (Figure 7B(i)).[151] For instance, a polymer-assisted plasmonic sensor was developed by hybridizing polyelectrolyte multilayers (PEMs) with gold nanoparticles to real-time monitor the binding of antigen−antibody on plasmonic sensors (Figure 7B(i)).[151] This hybrid film presented a stable and reliable nanoporous structure under physiological conditions and enhanced the surface area for bioconjugation and recognition.[151] Further, PEMs exhibited an antifouling property to prevent nonspecific binding of proteins and cells that enhanced detection sensitivity.[151] To utilize dynamic structure of polymers, thermoresponsive poly(*N*-isopropylacrylamide) (pNIPAAm)-based hydrogel was implemented as SPR sensors for rapid tuning of SPR signal (Figure 7B(ii)).[152] Here, an indium tin oxide microheater was embedded under the SPR sensor, and thus, rapid thermal response (i.e., swelling and collapse) of pNIPAAm was evaluated (Figure 7B(ii)).[152] Thermal response of pNIPAAm led to large refractive index changes and a high thermo-optical coefficient of $dn/dT = 2 \times 10^{-2}$ RIU/K.[152] Further, polymers can be modified with biorecognition elements for specific capture of target molecules, and thus, a 3D binding matrix can be developed for biosensing applications by utilizing dynamic and functional structure of polymers.[152,153,154]

Recently, the researchers have taken advantage of the plasmonic surface geometry for surface functionalization. Patterned nanoplasmonic structures with specialized geometries (e.g., holes and edges) exhibit a potential to be used for site-specific surface modifications that can increase the utility and specificity of nanoplasmonic platforms.[142b] Particularly, nanoplasmonic platforms employ noble metal surfaces (e.g., gold and silver) that can be modified using thiol chemistry to immobilize biorecognition elements.[155] Thiol chemistry also presents a broad range of variety in length, saturation degree, and terminal groups to preferably immobilize recognition elements (e.g., proteins, nucleotides, and carbohydrates) in plasmonically active zones.[142b,156] The thiol exchange process is an interesting strategy to selectively immobilize antibodies on the edges of triangular gold nanoplates that are used for LSPR sensing platform.[142a] The thiols located on the edges of the nanoplates are more attractive to exchange with the thiols in solution than the ones located on the flat surfaces of the nanoplates due to decreased steric hindrance at high-curvature sites.[142b,157] Other than patterned nanoplasmonic structures, hybrid noble metal layers can also be selectively functionalized for biosensing platforms (Figure 7C). Recently, nanohole arrays consisting of TiO_2/Au/TiO_2 films were specifically modified with poly-L-lysine−poly(ethylene glycol) (PLL−PEG) and thiolated PEG (HS-PEG) molecules (Figure 7C(i,ii)).[158] PLL−PEG selectively adsorbed to the TiO_2 layers (i.e., top and bottom layers), and HS-PEG covalently bound to gold layer (i.e., intersectional layer) (Figure 7C(iii)).[158] HS-PEG molecules were then functionalized with biotin for the selective detection of avidin on the hole sidewalls (Figure 7C(iii)).[158] This site-specific functionalization mechanism enabled the increase of the signal change per unit time for avidin−biotin binding nearly 20-fold (Figure 7C(iii)).[158] In the future, this functionalization strategy will play a key role for the improvement of sensitivity and the development of multiplex assays by enabling specific modifications on plasmonically active sites. Overall, surface functionalization is one of the key

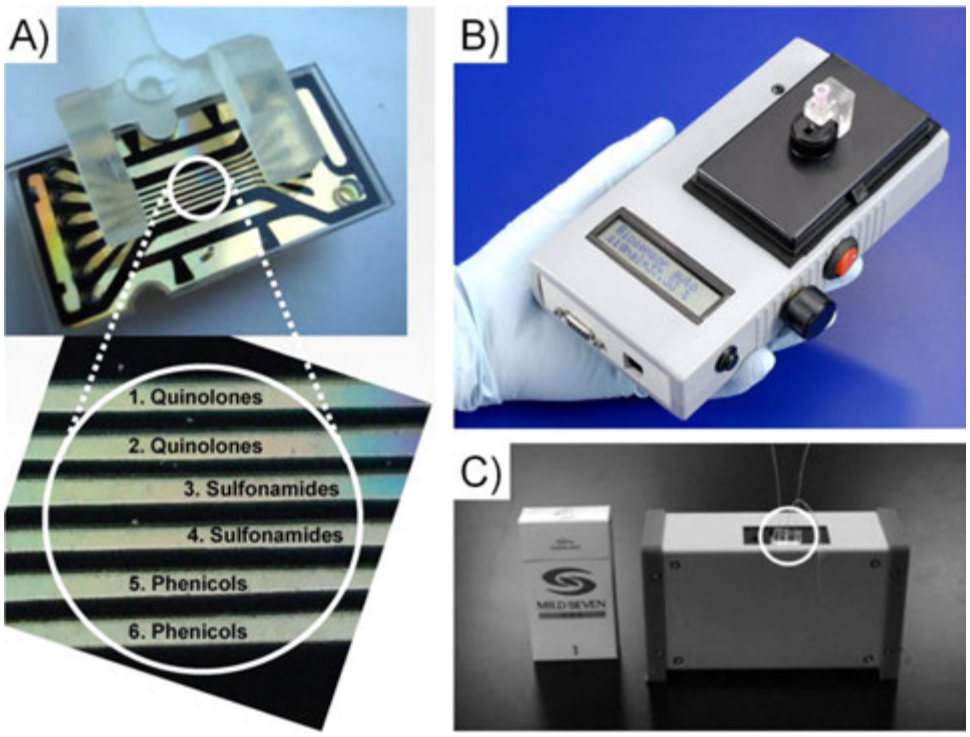

Figure 8. Portable SPR biosensor platforms. (A) A multichannel cartridge to be used for on-site antibiotic detection in milk samples. Reprinted with permission from ref 171. Copyright 2010 Elsevier. (B) Portable SPR biosensor prototype to be used with microfluidic chips. Reprinted with permission from ref 172. Copyright 2009 Elsevier. (C) Portable microfluidic-based device for cardiac marker detection. Reprinted with permission from ref 173. Copyright 2006 American Chemical Society.

parameters to develop a sensitive, reliable, and accurate biosensing platform.

5. APPLICATIONS OF PLASMONIC-BASED TECHNOLOGIES FOR POC: SPR, LSPR, AND SPRi

5.1. SPR

SPR has been used in a broad range of biosensing applications, including detection of bacteria, viruses, eukaryotic cells, nucleic acids, peptide nucleic acids, proteins, and drugs, and in monitoring of biomolecular interactions such as nucleic acid hybridization or protein−ligand interaction.[55]

Another important potential clinical application of SPR is in cancer diagnosis. Cancer is a significant problem both in the developed and developing world.[159] In 2008, ∼12.7 million cancer cases and 7.6 million cancer deaths occurred worldwide, and 56% of the cases and 64% of the deaths were reported in developing countries.[159] Although overall cancer incidence rates in developed countries are higher than those observed in developing countries, cancer mortality rates are usually similar between developed and developing countries.[159,160] Some of the most critical cancers in the developing world are female breast (27.3%), stomach (15.3%), lung (19.1%), colorectal (10.7%), and cervical (17.8%) cancers.[161] Early detection of cancer is a critical need in medicine, especially for cancer types such as breast, cervical, ovarian, and colorectal cancers.[160,162] Rapid available technologies to monitor early cancer markers supported by our advanced understanding of cancer and discovery of specific biomarkers will enhance the capabilities in cancer detection. Detection platform technologies could serve diverse clinical needs in early cancer detection and diagnosis (for instance by detecting circulating tumor cells[163]) or monitoring cancer treatment. In addition, these platforms could be inexpensive, rapid, portable, and easy to operate in developing countries as well as in developed settings, creating potentially broad screening tools for applicable cancer types. From a diagnostic perspective, detection of circulating biomarkers for cancer diagnosis is an interesting application of SPR-based detection platforms. For instance, cytokine interleukin-8 (IL-8) plays a crucial role in human cancer.[164] The differentiations in IL-8 expression level result in multiple human cancers, such as breast cancer, Hodgkin's lymphoma, and prostate cancer.[164] IL-8 concentration in saliva was shown to be elevated in oropharyngeal squamous cell carcinoma (OSCC) patients.[165] To detect the IL-8 concentrations in human saliva, a microfluidic SPR-based immunoassay platform was developed.[166] For this experiment, two monoclonal antibodies were used as a sandwich assay to detect different epitopes on the antigen (IL-8) in either buffer or saliva samples. This platform presented a 250 pM limit-of-detection in saliva environment.[166] IL-8 levels in healthy individuals saliva are 30 pM whereas the levels in oral cancer patients' saliva are 86 pM.[166] By preconcentrating the saliva in sample preparation steps, the system could potentially be used in diagnostics as well.

Another attractive biomarker detection experiment was performed for prostate-specific antigen (PSA). The increase in the levels of PSA (>4 ng/mL) in patient samples is one of the symptoms for possible prostate malignancy.[167] On the other hand, PSA has been reported as a potential marker for breast cancer in women.[168] To detect PSA levels a sandwich bioassay was developed.[169] Basically, anti-PSA antibodies were immobilized on the Au layer of the sensor surface. After the sampling, Au nanoparticles coated with a secondary antibody were applied to increase the SPR signal levels. In one

dx.doi.org/10.1021/cr4000623 | Chem. Rev. XXXX, XXX, XXX−XXX

experiment, 300 fM of PSA in PBS was detected using 20 nm Au nanoparticles.[169] In a similar study, different sizes of Au nanoparticles were evaluated in serum samples. For 20 and 40 nm Au nanoparticles, limit-of-detection was observed as 2.3 and 0.29 ng/mL (8.5 pM) in human serum, respectively.[170] The latter detection limit is reported to cover the threshold value required for diagnosing prostate cancer.[170]

A portable microfluidic-based SPR device was developed for analysis of antibiotics in milk. A disposable microfluidic cartridge incorporating six microchannels used in this device is illustrated in Figure 8A.[171] The chips were activated with self-assembled monolayers and then biofunctionalized to detect samples from fluoroquinolone, sulfonamide, and phenicol antibiotic families. The detection limit of the antibiotics in the former antibiotic families was around 2 μg/L with milk diluted by one-fifth in PBS, which is lower than the minimum required level (MRL) set by European Union regulations. The detection limit for the latter family was found to be 1.1 μg/L, which is slightly over the MRL of 0.3 μg/L. The platform does not require any sample preprocessing except dilution, and the process assay time is reported to take ~30 min per sample.

A prototype hand-held SPR-based device was developed and applied to biotoxin detection (Figure 8B).[172] The device incorporated a plastic flow cell as the detection medium, which can be replaced by a microfluidic chip in future versions. A photodiode array was used to capture the reflected light from the prism used in the Kretschmann configuration. The system detected ricin, a highly toxic protein, with a 200 ng/mL limit of detection compared to the 10 ng/mL performance of a commercial Biacore device. The main advantages of the system are its portability and battery operability, which are significant needs for POC diagnostics in resource-constrained settings.

Researchers have also followed the path of modifying some of the available commercial SPR devices for biosensing applications. For instance, SPR equipment (NTT Advanced, Tokyo, Japan) setup in the Kretschmann configuration was arranged to work with a polydimethylsiloxane (PDMS) microfluidic chip for the detection of B-type natriuretic peptide (BNP) as a cardiac biomarker.[173] The researchers developed a sensitive labeled immunoassay to be used in a portable SPR device. A detection level of 10 pg/mL in serum was demonstrated.[173] It is reported that the patient blood BNP levels range from ~20 pg/mL to 2 ng/mL; therefore, the platform could potentially be useful for clinical use.[173] This device is illustrated in Figure 8C. Another example to this strategy is demonstrated by the modification of a Spreeta 2000 device (Texas Instruments) to develop a portable 24-analyte biosensor.[174]

5.2. Localized Surface Plasmon Resonance

LSPR has been used in measurements of binding kinetics,[84a,175] conformational changes,[176] and molecular sensors,[177] and it is further exploited in nanoscale photonics.[178] The solution-phase nanoparticle sensing takes advantage of the dipole interactions between the nanoparticles when attached to target molecules. For example, when nanoparticles are hybridized to DNA targets and brought closer in solution, the LSPR modes of gold nanoparticles are coupled, and an enhanced extinction is observed. Distinguishing DNA target sequences that contain single nucleotide mismatches or deletions has been possible with this method, and an increase of sensitivity of 2 orders of magnitude compared to fluorescence-based assays has been reported.[179] Since this mode coupling is a function of distance between nanoparticles, it is possible to measure DNA strand lengths.[176a,180]

An alternative path is to synthesize arrays of nanoparticles on solid substrates and tailor their properties to optimize the extinction. Nanosphere lithography (NSL) is a rapid self-assembly chemical synthesis technique providing a cost-effective alternative to conventional lithographical techniques for creating periodic array structures. The challenge in this technique is the limitation of long-range defect-free layer production. In general, 10−100 μm^2 defect-free layers are possible.[181] Efforts to increase the defect-free synthesis range are continuing; e.g., large area defect-free nanohole arrays fabricated by NSL have been demonstrated.[182] Briefly, single or double layer ordered hexagonal arrays of polymer nanospheres are self-assembled on the substrate. Then, a metal layer is deposited on the nanosphere mask by thermal evaporation, pulsed laser deposition, or electron beam deposition. The interstices between the nanospheres allow some of the metal to reach to the substrate, creating an array of metal nanoparticles on the surface. Finally, the nanosphere layer(s) is/are removed by sonicating the sample in a solvent.[181] With variants of this technique, a wide variety of nanoshapes were fabricated in array format, including prisms, cubes, triangles, disks, and pyramidal structures.[80]

An earlier use of LSPR for clinical purposes has been through the detection and confirmation of a biomarker related to Alzheimer's disease.[183] LSPR spectroscopy was used to detect the interactions of the amyloid-derived diffusible ligand (ADDL) biomarkers with anti-ADDL antibodies. First, an array of Ag particles (~90 nm in width, ~25 nm in height) was synthesized on the substrate using the NSL technique described above. Then, the nanoparticles were activated with the first anti-ADDL antibody of a sandwich assay while also blocking the Ag particles for nonspecific binding. Samples were exposed to various concentrations of ADDLs. Finally, the sample was incubated in the second anti-ADDL antibody to improve the extinction signal. UV−vis spectroscopy was used to monitor the extinction signal. The experiments on cerebrospinal fluid from patients with Alzheimer's disease showed an LSPR extinction signal shift with respect to the control patients. The experiment supported previous observations of elevated ADDL concentrations in the cerebral fluids of patients with Alzheimer's disease and demonstrated the potential of LSPR in medical applications.

Further examples of LSPR biosensing were given in peptide nucleic acid−DNA hybridization,[184] label-free DNA biosensing,[185] streptavidin−biotin interactions on gold nanorods,[186] aptamer−protein interactions,[187] and in detection of *Escherichia coli*,[188] PSA,[189] serum p53 protein, which is involved in head and neck squamous cell carcinomas,[190] and p53 gene mutation.[191]

Further, LSPR has applications in cancer diagnosis. An LSPR experiment utilizing a microspectrometer to detect oral epithelial cancer cells has been demonstrated.[192] The researchers used two epithelial malignant cell lines of human oral squamous cell carcinoma, HOC 313 clone 8 and HSC 3, and one nonmalignant cell line, HaCaT, human keratinocytes. The LSPR spectra from colloidal gold nanoparticles conjugated to monoclonal antiepidermal growth factor receptor (anti-EGFR) antibodies after incubation in cell cultures with the HaCaT cell line and the two malignant oral epithelial cell lines were measured. LSPR scattering images were also acquired by dark-field microscopy and used to demonstrate that antibody

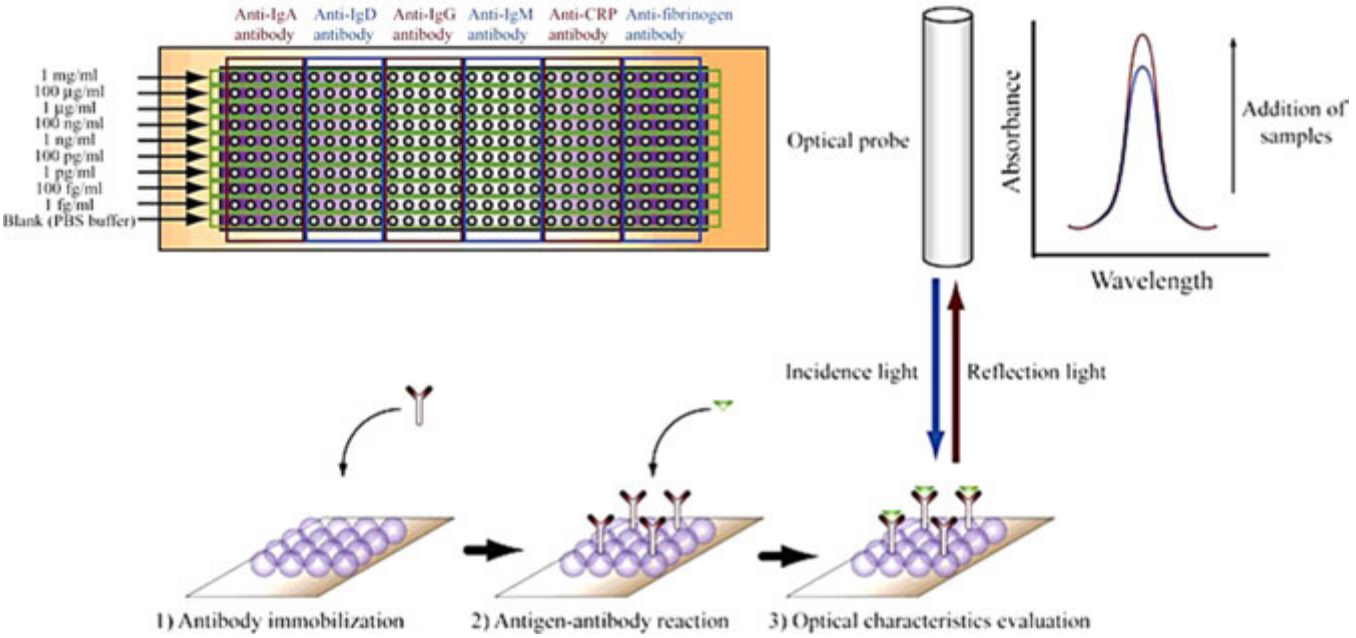

Figure 9. The distribution of six different antibodies corresponding to nine concentrations from 1 fg/mL to 1 mg/mL is shown along with the reflection-mode, intensity-based LSPR detection method. Reprinted with permission from ref 193. Copyright 2006 American Chemical Society.

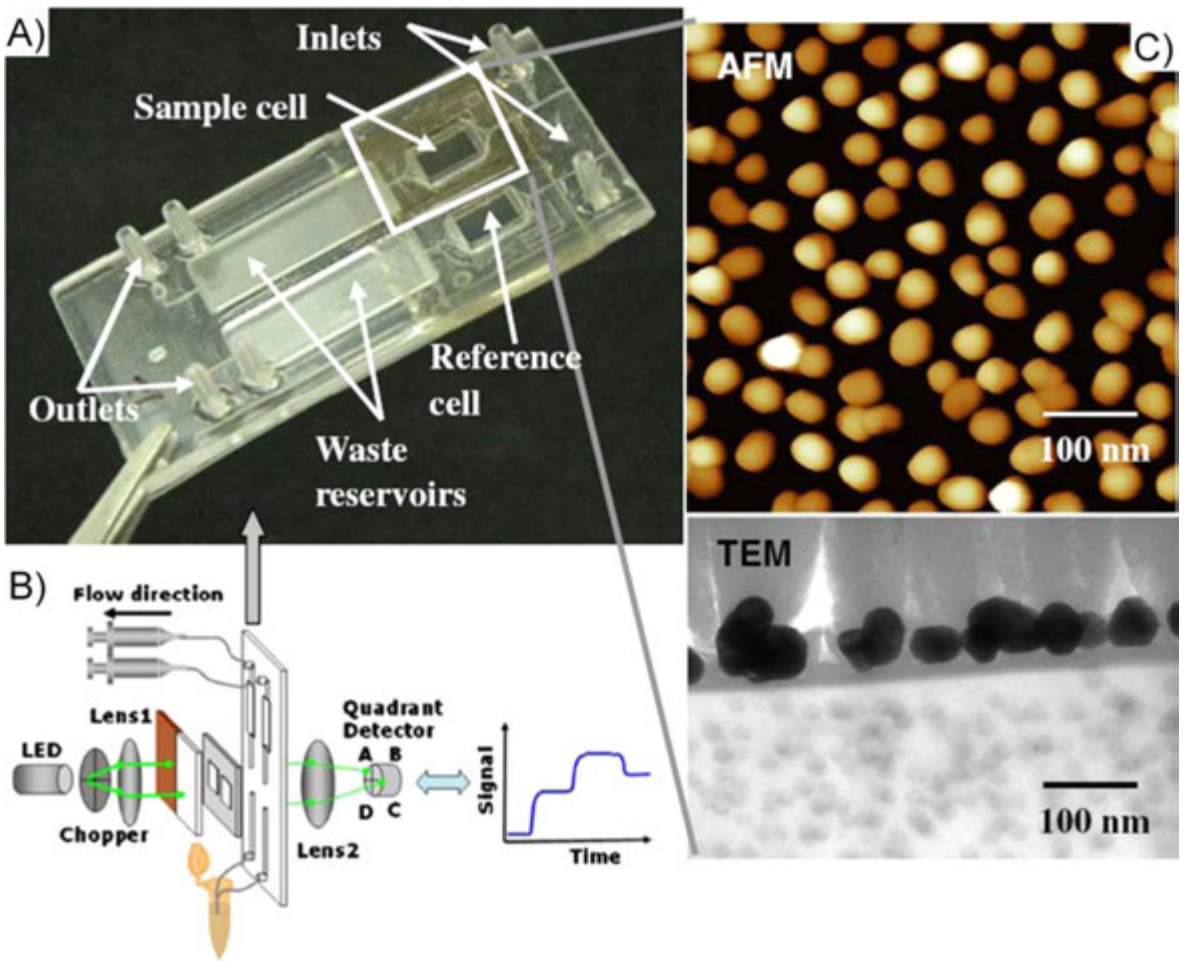

Figure 10. A microfluidic-based LSPR system. (A) The gold-nanosphere-coated LSPR channel and the control channel are positioned next to each other in the photograph of the microchip. (B) The experimental schematic indicating the LED light source, microfluidic chip, and photodetector. (C) Atomic force microscopy (AFM) and transmission electron microscopy (TEM) images of the nanoparticles on the chip. Reprinted with permission from ref 194. Copyright 2009 Springer.

dx.doi.org/10.1021/cr4000623 | *Chem. Rev.* XXXX, XXX, XXX–XXX

conjugated gold nanoparticles homogenously and specifically attached on the malignant cell surfaces, whereas the nanoparticles nonspecifically and randomly bound to HaCaT cell surfaces. Thus, both the extinction measurements and the dark-field images were shown to be potentially useful in cancer diagnostics.

Diagnostic LSPR applications for infectious diseases are also being developed. A recent LSPR application was reported to capture, detect, and quantify multiple HIV subtypes (A, B, C, D, E, G, and subtype panel) from unprocessed whole blood and phosphate-buffered saline (PBS) without any sample preprocessing.[56] In this study, polystyrene surfaces were first coated with poly-L-lysine molecules to immobilize gold nanoparticles. Then, specific surface chemistry was utilized to capture multiple HIV subtypes spiked in whole blood and PBS samples, and the limit-of-detection was observed down to 98 ± 39 virus copies/mL for HIV subtype D. Further, the nanoplasmonic platform was validated with eight HIV-infected anonymous discarded patient whole blood samples, and LSPR response was converted to viral load in order to correlate with gold standard method (i.e., RT-qPCR) using Bland–Altman analysis. This statistical analysis between the nanoplasmonic platform and RT-qPCR counts displayed that there was no evidence for a systematic bias for HIV-infected patient blood samples. To evaluate the repeatability of the presented platform, a repeatability parameter was defined as the percent variation in wavelength shift values for the same virus concentration, and the platform presented a high repeatability (up to 90%), sensitivity, and specificity to capture multiple HIV subtypes from unprocessed whole blood and whole blood samples from HIV-infected patients. This nanoplasmonic technology presented a versatile, broadly applicable platform, which is capable of detecting other pathogens with reasonably well-described biomarkers available, and could be performed at multiple settings including POC settings and primary care settings.

Microfluidic-based platforms are being developed for multiplexed analysis of various biomarkers. An LSPR-based multiarray nanochip for massively parallel detection was reported (Figure 9).[193] The nanochip was constructed by a core–shell structured nanoparticle layer. Surface-modified, 100-nm-diameter silica nanoparticles were sandwiched between two layers of gold deposited by thermal deposition. Glass slides were used as substrates for gold deposition. The bottom layer was made of 5-nm-thick chromium and 40-nm-thick gold layers, and the layer on top of the silica was made of a 30-nm-thick gold layer. Specific antibodies were then immobilized on the 300 spots each with a 100 nL volume, using a nanoliter dispensing system. In this work, six different antibodies on 50 spots each were immobilized. After 30 min incubation with six antigens of varying concentrations, immunoglobulins A, D, G, and M (IgA, IgD, IgG, and IgM); C-reactive protein (CRP); and fibrinogen were detected by an LSPR setup operating in the reflection mode. It should be noted that the measurements were absorbance intensity changes in the peak wavelength instead of the more common wavelength shifts. A sensitivity of 100 pg/mL for all proteins and a linear signal dependence up to 1 μg/mL were reported. This easy-to-operate, multiplexed, rapid technique has prospects in future POC technologies when applied to various biomarkers.

Another LSPR-based biosensor with fully integrated microfluidics is shown in Figure 10.[194] The platform comprises a gold-nanoparticle-coated quartz surface for the sensor channel and a blank quartz surface without nanoparticles serving as the reference channel. The diameter of gold nanoparticles was optimized with three-dimensional finite-difference time-domain (3-D FDTD) simulations. The gold nanoparticles were immobilized on the sample channel substrate by using silane modification. In this platform, the binding of biotin to antibiotin antibody was evaluated. The immobilization of biotin on a self-assembled monolayer of thiol and the following binding of antibiotin were monitored in real-time by the LSPR signal. A 530 nm LED was used as the light source, and a photodiode was used as the detector. The collimated and focused light incident on the sample channel excites LSPR modes of the gold nanoparticles, and the remaining light transmitted to the photodiode was used to collect real-time binding analysis data. A resolution of 10^{-4} in refractive index corresponding to an antibiotin detection limit of 270 ng/mL was achieved. The resolution of the microfluidic LSPR system was comparable to that of conventional LSPR biosensors.[73] Generalization of this system to other biomolecules is possible, and with a versatile and compact design, it has many prospects in various POC settings.

5.3. Surface Plasmon Resonance Imaging (SPRi)

The early demonstrations of SPRi aimed at providing better resolution over microscopic techniques such as phase contrast microscopy or interference contrast microscopy.[195] SPRi is a high-throughput optical detection method similar to the sensogram-based SPR techniques in principle, but the detection step allows imaging potentially tens of channels in parallel. A monochromatic or narrow-pass filtered light passing through a prism, which is typically configured in the Kretschmann configuration, is incident on the activated thin metal surface close to the surface plasmon resonance angle. Binding of the analytes will induce a refractive index change in a vicinity close to the metal, allowing for the incoming light to couple to the surface plasmon modes and lose some energy to the propagating surface plasmon polaritons. This energy loss will be observed as a change in the intensity of the reflected light. Since the binding to activated sites on the metal causes local refractive index changes, this spatial information will be transferred to the reflected light. Thus, the captured images will allow for temporal and spatial monitoring of surface binding events in a label-free setup, allowing for adsorption and desorption kinetic measurements and highly sensitive biorecognition experiments.[196]

Earlier reported work in this area was in analyzing nucleic acid hybridization, enzyme kinetics, and protein–DNA interactions.[197] Surface functionalization techniques for high-throughput array-based SPRi detection, involving carbohydrate–protein interactions, protein–peptide interactions, and protein–protein interactions, were developed.[198] RNA hybridization on DNA surface arrays was shown, at around 10 nM detection limit.[199] With enzyme amplification using RNase H, the detection limit was improved from 1 nM to ~1 fM for DNA hybridization on RNA microarrays.[200] The technique utilizes the fact that RNase H enzyme selectively and repeatedly destroys RNA from the DNA–RNA heteroduplexes on gold surfaces, releasing the DNA back into the solution and resulting in a six orders of magnitude improvement in the detection limit.

Enzyme reactions have been observed with SPRi, such as the base excision repair (BER) reaction and the activity of the DNA *N*-glycosylases enzyme. This enzyme is crucial in the major mechanism of the nucleobase error correction mechanism,

dx.doi.org/10.1021/cr4000623 | *Chem. Rev.* XXXX, XXX, XXX–XXX

since a decrease in its activity leads to carcinogenesis and aging.[201] An SPRi experiment reported the recognition of several damaged DNA nucleobases and the screening for inhibitors of DNA repair proteins.[202] Aptamers, natural or engineered nucleic acids and peptides, have also been used in conjunction with the SPRi technique. For instance, in aptamer–protein interaction studies, detection platforms for human factor IXa,[203] vascular endothelial growth factor,[204] and human immunoglobin E[205] were reported.

An SPRi system with a HeNe laser as a light source was developed to study the protein-binding kinetics of double-stranded DNA on a 10 × 12 array of planar gold surface. Using this system, a refractive index change of 1.8×10^{-5} RIU was observed.[206] The improvement of this system led to the detection of an effective refractive index change of 5×10^{-6} RIU on a 300 spot protein array with 200 μm spot size and 1 s temporal resolution.[207] Another SPRi system based on a tunable light source was shown to be sensitive to a refractive index change of 3×10^{-5} RIU.[208] The imaging technique was investigated with a polarization contrast approach to acquire high-contrast images. This was accomplished by filtering the light reflected from the inactive areas. This system showed a sensitivity of around 3×10^{-6} RIU in refractometric experiments, and the sensor could provide 64 simultaneous measurements with a limit of detection of 100 pM for 23-mer oligonucleotides.[209]

Recently, high-throughput and integrated microfluidic applications of SPRi have gained considerable attention. These systems provide the integration of various elements required for the on-chip applications. For example, a microfluidic chip with microchannels, microvalves, micropumps, flow sensors, and an on-chip temperature controller was developed with MEMS technology. The chip comprised three layers of PDMS, carrying these structures on a glass substrate. The system has been demonstrated through the detection of interaction between IgG and antirabbit IgG, and a detection limit of 1×10^{-4} mg/mL (0.67 nM) was observed.[210]

SPRi measurements of antibody arrays for larger molecules, such as mouse KIAA proteins (MW ~130 kDa)[211] and proteins in cell lysates,[212] bovine serum albumin (MW ~69 kDa), and bovine IgG (MW ~150 kDa),[213] were followed by measurements for lighter biomarkers (MW ~10 kDa). For instance, a high-density multiplexed antibody array was combined with the SPRi technique, to detect low molecular weight protein biomarkers (Figure 11).[214] One-step carbonyldiimidazole (CDI) surface chemistry was used to attach β_2-microglobulin (MW ~11.8 kDa) and cystatin C (MW 13.4 kDa) biomarkers on functionalized gold surfaces. The created antibody microarray comprised array element sizes between 750 μm and 200 μm. The SPRi system was able to detect these biomarkers with a sensitivity of down to ~1 nM.

A recent advance is the development of a microfluidic chip for immunoassay-based SPRi.[215] The system, shown in Figure 12, was comprised of two levels. The "flow channel" level was comprised of a crossed-flow architecture, allowing for loading two sets of reagents simultaneously. A second level, the "control channel", hosted microfluidic pumps for controlling the liquid flow in the flow channel. The lower layer crossed-channels have a width of 100 μm and a height of ~10 μm, and their intersection is located over surface-activated gold spots with 250 μm diameters and ~50 nm thickness, where the immunoreactions take place. These layers were fabricated through photolithographic techniques on PDMS and were

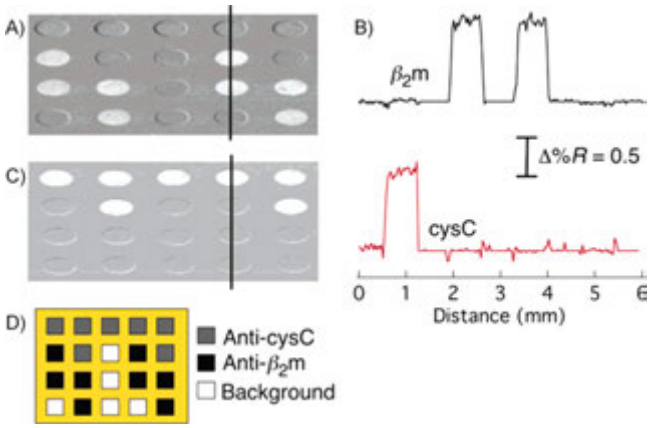

Figure 11. SPRi detection of 50 nM β_2-microglobulin (β_2m) and 100 nM cystatin C (cysC). (A and C) Images for β_2m and cysC detection, respectively. (B) The line profiles indicated in parts A and C show signal only in the corresponding channels where the antibodies were positioned. (D) Map of the antibodies and control channels used in parts A and C. Reprinted with permission from ref 214. Copyright 2006 American Chemical Society.

attached to each other with the dipping–attaching method.[216] In the setup, p-polarized incoming light (625 nm) passes through a prism and hits on the gold areas. The reflected light emerges from the prism and is collected by a home-made digital imaging device. To demonstrate the detection performance of the chip, first a one-step immunoassay examined the binding of anti-biotin antibodies to biotinylated bovine serum albumin (biotin–BSA), as an antibody–antigen pair. A group of biotin–BSA/BSA solutions with different concentrations was injected in horizontal channels, resulting in adsorption of biotin–BSA/BSA on the gold surfaces. Then, known concentrations of anti-biotin solutions were injected in the vertical channels, creating immunoreactions with the immobilized biotin–BSA. The immunocomplex formation was related to both the biotin–BSA concentration on the surface and to the anti-biotin antibody. Real-time immunoassay imaging allowed for monitoring of each immunoreaction in about 10 min, and the system attained a sub-nanomolar detection limit. Next, a two-level immunoassay was utilized for signal amplification. Another antibody, anti-goat IgG antibody, labeled with gold nanoparticles was delivered to the gold spots. This improved the limit of detection down to ~40 pM. With its small instrument dimensions of ~2–3 cm and with less than 100 pM detection performance as a microscale platform, this SPR imaging system has potential for future POC applications.

To increase the unit addressing capability in a crossed-flow geometry, a microfluidic chip with individually addressable chambers was developed (Figure 13).[217] The design allows for parallel interrogation of multiple analytes with multiple ligands on an SPRi setup. The chip has two levels similar to the microchip developed in ref 215. The lower level contains the flow channels (100 μm wide by 10 μm high) and the upper level contains microvalves (100 μm wide by 150 μm long) isolating and controlling the liquid flow and a micropump to pump the liquid. The chip is comprised of six columns and an array of 11 groups each with four chambers, totaling 264 chambers. To load an individual chamber, first the liquid is gated to a four chamber group and then four chamber valves open or close to address the liquid to an individual chamber. After loading the required chambers, the valves for those

dx.doi.org/10.1021/cr4000623 | Chem. Rev. XXXX, XXX, XXX–XXX

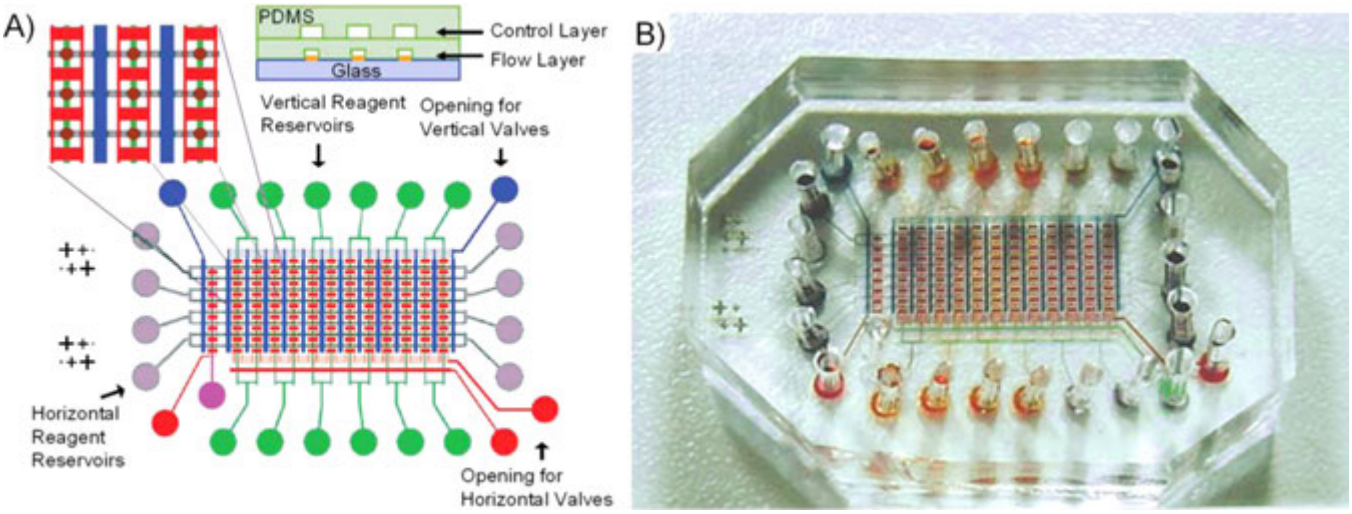

Figure 12. A microfluidic-based SPRi platform. (A) Schematic of the microchip for the SPRi experiment. The lower layer is where the immunoreactions take place, and the upper layer controls the fluid flow by microfluidic pumps. (B) The microfluidic device with dyed fluids to illustrate the microchannels. Figures are courtesy of Prof. Richard N. Zare.

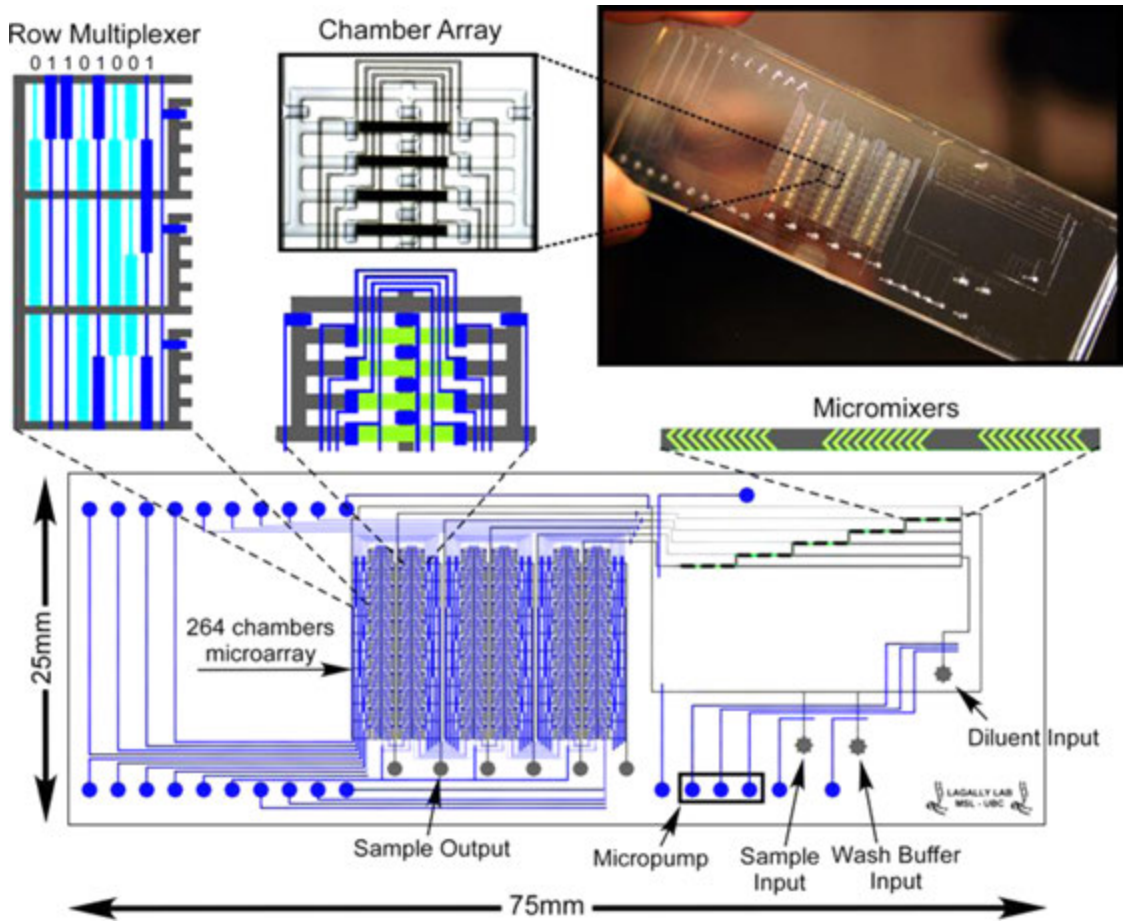

Figure 13. Layout of the element addressable microdevice for SPRi experiments, depicting the 264 chamber microarray, accessed by various features, such as a micropump, microvalves, micromixers, input/output channels, and a row multiplexer. A detailed microarray is shown along the photograph of the microfluidic chip. Figures are courtesy of Prof. Eric T. Lagally.

chambers are closed and the remaining liquid is washed out. With this method, up to 264 different ligands can be immobilized in the system. The chip also comprises a serial dilution network for analytes, allowing dilutions of samples up to six different concentrations for interrogations.

To test the performance of the chip, a human α-thrombin immunoassay was conducted. The biotinylated human α-thrombin was immobilized in a predetermined manner, taking advantage of the element-addressability of chambers. Antihuman α-thrombin antibody was injected at different concen-

dx.doi.org/10.1021/cr4000623 | *Chem. Rev.* XXXX, XXX, XXX–XXX

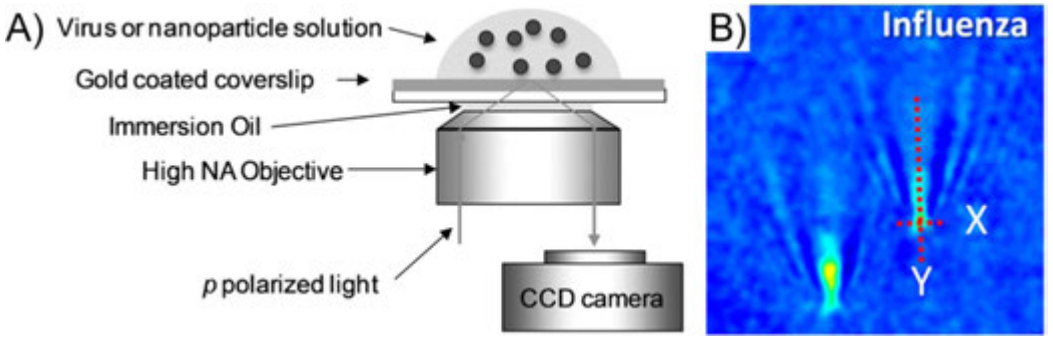

Figure 14. SPRi system used for individual virus particle imaging. (A) The schematic for the SPRi experiment utilizing an objective in the Kretschmann configuration and an inverted microscope. (B) SPR images of the influenza A virus in PBS buffer. Reprinted with permission from ref 218. Copyright 2010 National Academy of Sciences.

trations. The binding of the antibody and its kinetics were successfully observed in the SPRi sensogram data. Further, two immunoassays were simultaneously performed to demonstrate the multiplexed nature of the chip. Human factor IX proteins were immobilized in 44 element-addressable chambers and human α-thrombin proteins were immobilized in another set of 44 element-addressable chambers. In addition, using fluorescent-labeled antibodies in conjunction with SPRi sensograms, the ability to recover bound species from individual chambers was demonstrated. This SPRi device architecture could be used in future high-throughput medical applications.

An important SPRi advance recently reported individual virus particle detection. An SPRi device was developed, based on the Kretschmann configuration, that incorporated a high numerical aperture (NA = 1.65) objective to image single viruses.[218] An SPR chip was placed on the objective with index matching oil, as shown in Figure 14. Then, 632.8 nm of laser light from a HeNe laser or 680 nm superluminescence diode light was p-polarized and inserted in the optical path to excite surface plasmons on the gold surface. The SPRi images allowed the imaging of individual influenza A virus binding events on antibody-functionalized gold surfaces. Nanoparticles of known sizes and estimated refractive indices were used for calibration curves, intensity−volume curves were plotted, and volumetric information for the influenza A virus was extracted. Using the known density of influenza A virus, diameter of the virus was calculated as 109 ± 13 nm, corresponding to a mass of 0.80 ± 0.35 fg. Human cytomegalovirus (HCMV) was also studied with the setup and the virus diameter was extracted as 218 ± 10 nm, corresponding to a mass of 6.5 ± 0.8 fg.

6. CONCLUSION AND FUTURE OUTLOOK

Plasmonic-based biosensor technologies can be used in different economic settings for diagnostic testing, such as (i) "high-income, centralized"; (ii) "high-income, POC"; (iii) "low-income, centralized"; and (iv) "low-income, POC".[4] High-income, POC is exemplified by bedside diagnostic tests and disaster or bioemergency response in developed countries. Low-income, POC can be rural health clinics with basic infrastructure or isolated village health service providers. These conditions impose different levels of constraints on diagnostic device engineering and design. For instance, material choice, storage, transportation, fluid control, sample mixing, and disposal need to be tailored for targeted POC conditions and applications. Interdisciplinary research efforts are beneficial to address all these issues for diagnostic device design at the POC.

The research efforts in developing technological platforms for POC are positioned at the cross-roads of multiple disciplines. "Convergence" of multiple research fields is emerging as a new paradigm in science, indicating the synergy between engineering, physical sciences, and life sciences.[219] Cross-disciplinary pollination among chemistry, biology, electrical engineering, optics, and biotechnology is transforming each field and creating new ways of doing engineering and performing fundamental life science research, as well as providing new potential clinical applications. The LOC devices with integrated nanoplasmonic and microfluidic components, inexpensive fabrication techniques, and reliable read-outs for portable commercial POC platforms will be a part of this transformation. We believe that the progress in the microfluidics field converging with optics, electronics, and bioengineering will greatly enhance the human health through generating inexpensive, rapid, portable, and sensitive platform technologies.

Future robust and easy-to-operate POC testing systems will also support the personalized medicine efforts.[220] For instance, the development of reliable bedside technologies for medical diagnosis of infectious diseases would have a great impact in disease monitoring and control. The current bedside testing devices are exemplified by disposable immunochromatographic strip tests.[7,221] Integrated microfluidic−plasmonic technologies can be potentially utilized at the bedside for various diseases, including examples such as hepatitis, sepsis, pneumonia, cancer, and AIDS. We envision that these technologies will play an important role in infectious disease detection and monitoring at the POC, bedside, and primary care settings.

Another area with an unmet diagnostic need is immunodiagnostics.[222] Detection of protein markers can help diagnose conditions such as cancer, metabolic diseases, or cardiovascular diseases. Technologies sensitive to these proteins can be used for monitoring disease progression, therapy, or early diagnosis.[222] Other areas that could potentially benefit from the development of microfluidic POC platforms include toxin monitoring, food safety, drug discovery, and proteomics research.[18a]

One of the challenges from a POC perspective has been transferring prototype plasmonic-based technologies from the laboratory settings to clinical use. In the case of LSPR, development of sensitive, portable, and inexpensive spectrometers will assist this transformation. Portable spectrometers are already becoming available in the market.[223] Periodic or quasi-periodic metal nanoarrays, nanoholes, and nanoparticles with engineered electromagnetic field enhancement properties can

dx.doi.org/10.1021/cr4000623 | Chem. Rev. XXXX, XXX, XXX−XXX

provide enhanced localized surface plasmon excitation and detection capabilities.[71,224] The translation of LSPR technologies depends on their compatibility with batch-fabrication to enable inexpensive devices. Currently, nanohole or similar periodic nanoarray systems require expensive lithographic methods that are limited by throughput. Some of the recent LSPR approaches that use self-assembly of gold nanoparticles, which are compatible with 96-well and microfluidic chip systems, are promising for applications in infectious disease and early cancer detection both in developed and developing settings.[56] Therefore, future advances in nanotechnology are likely to provide significant improvements in LSPR-based biomedical devices.

SPR technology has been commercialized, most notably by Biacore's and KSV Instruments' SPR series. The technological challenges effecting SPR-based technologies for POC diagnostic applications include generating substrates that will present reproducible results from batch to batch, integrating the systems for portability, and adapting the systems for use with bodily fluids. Developing diagnostic platforms that will operate at the POC will require adapting SPR-based technologies to be used as a versatile, inexpensive, and portable platform. Flexible substrates such as paper-based printed chips or microfluidic cartridges operating with portable readers will help translating SPR devices. Further, the electronics industry is consistently creating more affordable and rapid optical detectors and improved networked devices. Recently, smartphones spread around the world rapidly. Considering the possibilities of using built-in sensors or cameras in smart phones as a part of integrated microfluidics platforms, it is conceivable that the next-generation SPR devices will penetrate into global markets and households. In particular, smartphone penetration in Africa can be leveraged for POC device distribution, where these devices can be utilized as a reader component for biosensing applications.[225,226,227]

We expect that microfluidic platforms, plasmonic technologies, and surface functionalization techniques integrated in reliable and sensitive lab-chip applications will continue to serve clinical needs and patients. The development of immunoassays and further integration of these assays with microfluidic technologies and emerging portable optical technologies have the potential to enable applications that will benefit both the resource-constrained and the developed world settings, targeting real world clinical problems and diseases including cancer and infectious diseases.

AUTHOR INFORMATION

Corresponding Author

*E-mail: utkan@stanford.edu.

Present Address

[⊥]Bilkent University, Ultrafast Optics and Lasers Group, Department of Physics, Cankaya, Ankara 06800, Turkey

Notes

Dr. Utkan Demirci is a founder of, and has an equity interest in, DxNow, a company that is developing microfluidic and imaging technologies for point-of-care diagnostic solutions. Dr. Utkan Demirci's interests were viewed and managed by the Brigham and Women's Hospital and Partners HealthCare in accordance with their conflict of interest policies.

Biographies

Onur Tokel, PhD, is a Postdoctoral Research Fellow in Medicine at Harvard Medical School and Division of Biomedical Engineering and Division of Infectious Diseases at Brigham and Women's Hospital. He received his B.S degree from Bilkent University, Turkey in Electrical Engineering, and his M.S. degree from Cornell University in Applied Physics. He has worked as a visiting scholar at the Advanced Light Source, Lawrence Berkeley National Laboratory and helped set-up the Houston Lab at Georgia Institute of Technology, Atlanta. He holds a Ph.D. from Cornell University in Applied Physics. His research has been in the area of fundamental light−matter interactions, laser and molecular imaging. These technologies were used for a greater understanding of laser−molecule interactions at the quantum mechanical level. He is currently interested in the integration of optical technologies and microfluidic technologies for applications in inexpensive, robust and portable health technologies. He is developing lab-chip systems for diagnostics and immunodiagnostics for applications in resource-constrained settings as well as for primary care.

Fatih Inci, Ph.D., is a Postdoctoral Research Fellow at Stanford University School of Medicine, Canary Center at Stanford for Cancer Early Detection. He received his bachelor's degree in Molecular Biology and Genetics Department in 2007 from Istanbul University, Turkey, and his Ph.D. degree in Molecular Biology−Genetics and Biotechnology Department in 2013 from Istanbul Technical University, Turkey. He also has several appointments as a visiting researcher/student/research fellow in Biology Department, University of Groningen, Netherlands, School of Biotechnology and Biomolecular Sciences, University of New South Wales, Australia, Institute for Nanoscale Technology, University of Technology Sydney, Australia, Medicine, Harvard Medical School, and Division of Biomedical Engineering, Brigham and Women's Hospital, United States. He has focused on the point-of-care diagnostic technologies, microfluidics,

dx.doi.org/10.1021/cr4000623 | Chem. Rev. XXXX, XXX, XXX−XXX

lab-on-a-chip platforms, nanoplasmonic-based biosensors, optical tweezers, artificial lipid membranes, controlled drug delivery systems, smart polymers, surface chemistry approaches, and tissue engineering applications. He is currently developing microfluidic and lab-chip platforms integrated nanoplasmonic platforms for diagnostics applications in resource-constrained settings. His studies have been recognized by several esteemed corporations, including European Molecular Biology Organization—European Science Foundation (EMBO—ESF), Turkey Scientific and Technological Research Society (TUBITAK), Istanbul University, and Istanbul Technical University. Additionally, he has published original research articles, reviews, and book chapters at many prestigious peer-reviewed journals in nanomedicine as well as in biotechnology/bioengineering journals, including *ACS Nano*, *Biotechnology Advances*, *Lab on a Chip*, *Small*, *Biomacromolecules*, and *International Journal of Nanomedicine*.

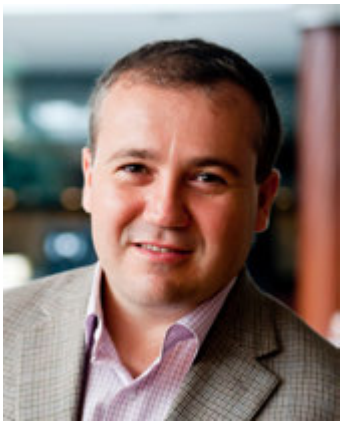

Utkan Demirci, Ph.D., is an Associate Professor at Stanford University School of Medicine, Canary Center at Stanford for Cancer Early Detection. He received his bachelor's degree in Electrical Engineering (Summa Cum Laude) in 1999 from the University of Michigan, An, an Arbor, his master's degrees in Electrical Engineering in 2001 and in Management Science and Engineering in 2005 from Stanford University, and his doctorate in Electrical Engineering in 2005, also from Stanford University. His current work involves applying nano- and microscale technologies to manipulate cells in nanoliter volumes, with applications in infectious disease diagnostics and monitoring, cell encapsulation and assembly for cryobiology, tissue engineering, and regenerative medicine. His research interests include the applications of microelectromechanical systems (MEMS) and acoustics in medicine. Dr. Demirci has authored over 80 peer-reviewed journal publications in journals, including *Nature Communications*, *Nature Materials*, *PNAS*, *Advanced Materials*, and *Lab on a Chip*, more than 100 conference abstracts and proceedings, and 12 book chapters and has edited a book on point of care diagnostics. His work has been highlighted in *Wired* magazine, *Nature Photonics*, *Nature Medicine*, *MIT Technology Review* magazine, *AIP News*, *BioTechniques*, and *Biophotonics*. He has given over 100 national and international presentations, including invited keynotes at various academic, governmental, and industrial institutions.

ACKNOWLEDGMENTS

We would like to acknowledge NIH RO1 AI093282, NIH RO1 A1081534, NIH U54EB15408, and NIH R21 AI087107. We also thank Brigham and Women's Hospital (BWH) Biomedical Research Institute Translatable Technologies & Care Innovation Award. We would also like to thank the illustrators, Yusuf Yesil for table of content figure and Simin Ecem Yildiz for Figure 4.

REFERENCES

(1) Yager, P.; Domingo, G. J.; Gerdes, J. *Annu. Rev. Biomed. Eng.* **2008**, *10*, 107.
(2) Sachs, J.; Malaney, P. *Nature* **2002**, *415*, 680.
(3) (a) Wang, S.; Xu, F.; Demirci, U. *Biotechnol. Adv.* **2010**, *28*, 770. (b) Wang, S.; Inci, F.; De Libero, G.; Singhal, A.; Demirci, U. *Biotechnol. Adv.* **2013**, *31*, 438.
(4) Chin, C. D.; Linder, V.; Sia, S. K. *Lab Chip* **2007**, *7*, 41.
(5) Daar, A. S.; Thorsteinsdottir, H.; Martin, D. K.; Smith, A. C.; Nast, S.; Singer, P. A. *Nat. Genet.* **2002**, *32*, 229.
(6) Diamond, J. M. *Guns, Germs, and Steel: The Fates of Human Societies*; Norton: New York, 2005.
(7) Yager, P.; Edwards, T.; Fu, E.; Helton, K.; Nelson, K.; Tam, M. R.; Weigl, B. H. *Nature* **2006**, *442*, 412.
(8) Tasoglu, S.; Gurkan, U. A.; Wang, S.; Demirci, U. *Chem. Soc. Rev.* **2013**, *42*, 5788.
(9) Mabey, D.; Peeling, R. W.; Ustianowski, A.; Perkins, M. D. *Nat. Rev. Microbiol.* **2004**, *2*, 231.
(10) Ozbay, E. *Science* **2006**, *311*, 189.
(11) Fan, X. D.; White, I. M.; Shopova, S. I.; Zhu, H. Y.; Suter, J. D.; Sun, Y. Z. *Anal. Chim. Acta* **2008**, *620*, 8.
(12) (a) Qavi, A. J.; Washburn, A. L.; Byeon, J. Y.; Bailey, R. C. *Anal. Bioanal. Chem.* **2009**, *394*, 121. (b) Yanik, A. A.; Huang, M.; Kamohara, O.; Artar, A.; Geisbert, T. W.; Connor, J. H.; Altug, H. *Nano Lett.* **2010**, *10*, 4962. (c) Gao, Y.; Gan, Q.; Xin, Z.; Cheng, X.; Bartoli, F. J. *ACS Nano* **2011**, *5*, 9836.
(13) (a) Monat, C.; Domachuk, P.; Eggleton, B. J. *Nat. Photon.* **2007**, *1*, 106. (b) Guo, Y.; Oo, M. K. K.; Reddy, K.; Fan, X. *ACS Nano* **2011**, *6*, 381. (c) Chin, C. D.; Linder, V.; Sia, S. K. *Lab Chip* **2007**, *7*, 41.
(14) (a) Alyassin, M. A.; Moon, S.; Keles, H. O.; Manzur, F.; Lin, R. L.; Haeggstrom, E.; Kuritzkes, D. R.; Demirci, U. *Lab Chip* **2009**, *9*, 3364. (b) Gurkan, U. A.; Tasoglu, S.; Akkaynak, D.; Avci, O.; Unluisler, S.; Canikyan, S.; MacCallum, N.; Demirci, U. *Adv. Healthcare Mater.* **2012**, *1*, 661. (c) Wang, S.; Sarenac, D.; Chen, M. H.; Huang, S.-H.; Giguel, F. F.; Kuritzkes, D. R.; Demirci, U. *Int. J. Nanomed.* **2012**, *7*, 5019.
(15) Whitesides, G. M. *Nature* **2006**, *442*, 368.
(16) Ivnitski, D.; Abdel-Hamid, I.; Atanasov, P.; Wilkins, E. *Biosens. Bioelectron.* **1999**, *14*, 599.
(17) Brolo, A. G. *Nat. Photonics* **2012**, *6*, 709.
(18) (a) Mayer, K. M.; Hafner, J. H. *Chem. Rev.* **2011**, *111*, 3828. (b) Piliarik, M.; Homola, J. *Opt. Express* **2009**, *17*, 16505.
(19) (a) Ross, B. M.; Tasoglu, S.; Lee, L. P. *Proc. SPIE* **2009**, 739422. (b) Premasiri, W. R.; Sauer-Budge, A. F.; Lee, J. C.; Klapperich, C. M.; Ziegler, L. D. *Spectroscopy* **2013**, *28*, 52.
(20) Stiles, P. L.; Dieringer, J. A.; Shah, N. C.; Van Duyne, R. R. *Annu. Rev. Anal. Chem.* **2008**, *1*, 601.
(21) Premasiri, W. R.; Moir, D. T.; Klempner, M. S.; Krieger, N.; Jones, G., 2nd; Ziegler, L. D. *J. Phys. Chem. B* **2005**, *109*, 312.
(22) Shanmukh, S.; Jones, L.; Driskell, J.; Zhao, Y. P.; Dluhy, R.; Tripp, R. A. *Nano Lett.* **2006**, *6*, 2630.
(23) (a) Barhoumi, A.; Zhang, D.; Tam, F.; Halas, N. J. *J. Am. Chem. Soc.* **2008**, *130*, 5523. (b) Neumann, O.; Zhang, D. M.; Tam, F.; Lal, S.; Wittung-Stafshede, P.; Halas, N. J. *Anal. Chem.* **2009**, *81*, 10002.
(24) Han, X. X.; Zhao, B.; Ozaki, Y. *Anal. Bioanal. Chem.* **2009**, *394*, 1719.
(25) Bantz, K. C.; Meyer, A. F.; Wittenberg, N. J.; Im, H.; Kurtulus, O.; Lee, S. H.; Lindquist, N. C.; Oh, S. H.; Haynes, C. L. *Phys. Chem. Chem. Phys.* **2011**, *13*, 11551.
(26) (a) Nie, S. M.; Emery, S. R. *Science* **1997**, *275*, 1102. (b) Kneipp, K.; Wang, Y.; Kneipp, H.; Perelman, L. T.; Itzkan, I.; Dasari, R.; Feld, M. S. *Phys. Rev. Lett.* **1997**, *78*, 1667. (c) Santos, D. P. d.; Andrade, G. F. S.; Temperini, M. L. A.; Brolo, A. G. *J. Phys. Chem. B* **2009**, *113*, 17737.
(27) Fan, M.; Wang, P.; Escobedo, C.; Sinton, D.; Brolo, A. G. *Lab Chip* **2012**, *12*, 1554.
(28) (a) Lin, V. S.-Y.; Motesharei, K.; Dancil, K.-P. S.; Sailor, M. J.; Ghadiri, M. R. *Science* **1997**, *278*, 840. (b) Lopez, C. A.; Daaboul, G. G.; Vedula, R. S.; Ozkumur, E.; Bergstein, D. A.; Geisbert, T. W.;

Fawcett, H. E.; Goldberg, B. B.; Connor, J. H.; Unlu, M. S. *Biosens. Bioelectron.* **2011**, *26*, 3432.
(29) Kumeria, T.; Kurkuri, M. D.; Diener, K. R.; Parkinson, L.; Losic, D. *Biosens. Bioelectron.* **2012**, *35*, 167.
(30) Pröll, F.; Möhrle, B.; Kumpf, M.; Gauglitz, G. *Anal. Bioanal. Chem.* **2005**, *382*, 1889.
(31) Choi, H. W.; Takahashi, H.; Ooya, T.; Takeuchi, T. *Anal. Methods* **2011**, *3*, 1366.
(32) Fechner, P.; Proll, F.; Albrecht, C.; Gauglitz, G. *Anal. Bioanal. Chem.* **2011**, *400*, 729.
(33) (a) Vollmer, F.; Arnold, S. *Nat. Methods* **2008**, *5*, 591. (b) Santiago-Cordoba, M. A.; Boriskina, S. V.; Vollmer, F.; Demirel, M. C. *Appl. Phys. Lett.* **2011**, *99*, 073701.
(34) Armani, A. M.; Kulkarni, R. P.; Fraser, S. E.; Flagan, R. C.; Vahala, K. J. *Science* **2007**, *317*, 783.
(35) (a) Joannopoulos, J. D. *Photonic Crystals: Molding the Flow of Light*, 2nd ed.; Princeton University Press: Princeton, NJ, 2008. (b) Sridharan, D.; Bose, R.; Kim, H.; Solomon, G. S.; Waks, E. *Opt. Express* **2011**, *19*, 5551.
(36) Cunningham, B. T. *JALA (1998-2010)* **2010**, *15*, 120.
(37) Pineda, M. F.; Chan, L. L. Y.; Kuhlenschmidt, T.; Choi, C. J.; Kuhlenschmidt, M.; Cunningham, B. T. *IEEE Sens. J.* **2009**, *9*, 470.
(38) Shafiee, H.; Lidstone, E. A.; Jahangir, M.; Inci, F.; Hanhauser, E.; Henrich, T. J.; Kuritzkes, D. R.; Cunningham, B. T.; Demirci, U. *Sci. Rep.* **2014**, *4*, 4116 DOI: DOI: 10.1038/srep04116.
(39) Chevaliez, S.; Bouvier-Alias, M.; Laperche, S.; Pawlotsky, J.-M. *J. Clin. Microbiol.* **2008**, *46*, 1716.
(40) Lee, M.; Fauchet, P. M. *Opt. Express* **2007**, *15*, 4530.
(41) Chan, L. L.; Gosangari, S. L.; Watkin, K. L.; Cunningham, B. T. *Apoptosis* **2007**, *12*, 1061.
(42) Lisdat, F.; Schäfer, D. *Anal. Bioanal. Chem.* **2008**, *391*, 1555.
(43) Cheng, X.; Liu, Y.-s.; Irimia, D.; Demirci, U.; Yang, L.; Zamir, L.; Rodriguez, W. R.; Toner, M.; Bashir, R. *Lab Chip* **2007**, *7*, 746.
(44) (a) Dharuman, V.; Grunwald, T.; Nebling, E.; Albers, J.; Blohm, L.; Hintsche, R. *Biosens. Bioelectron.* **2005**, *21*, 645. (b) Li, Y.; Wark, A. W.; Lee, H. J.; Corn, R. M. *Anal. Chem.* **2013**, *85* (8), 4129 DOI: 10.1021/ac4002657. (c) Kafka, J.; Pänke, O.; Abendroth, B.; Lisdat, F. *Electrochim. Acta* **2008**, *53*, 7467.
(45) (a) Varshney, M.; Li, Y. *Biosens. Bioelectron.* **2007**, *22*, 2408. (b) Maalouf, R.; Fournier-Wirth, C.; Coste, J.; Chebib, H.; Saïkali, Y.; Vittori, O.; Errachid, A.; Cloarec, J.-P.; Martelet, C.; Jaffrezic-Renault, N. *Anal. Chem.* **2007**, *79*, 4879.
(46) Herzog, G.; Arrigan, D. W. M. *Analyst* **2007**, *132*, 615.
(47) Shafiee, H.; Jahangir, M.; Inci, F.; Wang, S.; Willenbrecht, R. B.; Giguel, F. F.; Tsibris, A. M.; Kuritzkes, D. R.; Demirci, U. *Small* **2013**, *9*, 2553.
(48) (a) Binnig, G.; Quate, C. F.; Gerber, C. *Phys. Rev. Lett.* **1986**, *56*, 930. (b) Muller, D. J.; Dufrene, Y. F. *Nat. Nanotechnol.* **2008**, *3*, 261.
(49) Nugaeva, N.; Gfeller, K. Y.; Backmann, N.; Lang, H. P.; Duggelin, M.; Hegner, M. *Biosens. Bioelectron.* **2005**, *21*, 849.
(50) Zhang, J.; Lang, H. P.; Huber, F.; Bietsch, A.; Grange, W.; Certa, U.; McKendry, R.; Guntgerodt, H. J.; Hegner, M.; Gerber, C. *Nat. Nanotechnol.* **2006**, *1*, 214.
(51) Mukhopadhyay, R.; Sumbayev, V. V.; Lorentzen, M.; Kjems, J.; Andreasen, P. A.; Besenbacher, F. *Nano Lett.* **2005**, *5*, 2385.
(52) Fritz, J.; Baller, M. K.; Lang, H. P.; Rothuizen, H.; Vettiger, P.; Meyer, E.; Guntherodt, H. J.; Gerber, C.; Gimzewski, J. K. *Science* **2000**, *288*, 316.
(53) Burg, T. P.; Godin, M.; Knudsen, S. M.; Shen, W.; Carlson, G.; Foster, J. S.; Babcock, K.; Manalis, S. R. *Nature* **2007**, *446*, 1066.
(54) (a) Tao, N. J.; Boussaad, S.; Huang, W. L.; Arechabaleta, R. A.; D'Agnese, J. *Rev. Sci. Instrum.* **1999**, *70*, 4656. (b) Slavík, R.; Homola, J. *Sens. Actuators, B* **2007**, *123*, 10.
(55) Homola, J. *Chem. Rev.* **2008**, *108*, 462.
(56) Inci, F.; Tokel, O.; Wang, S.; Gurkan, U. A.; Tasoglu, S.; Kuritzkes, D. R.; Demirci, U. *ACS Nano* **2013**, *7*, 4733.
(57) Nie, S.; Emory, S. R. *Science* **1997**, *275*, 1102.
(58) Ozkumur, E.; Needham, J. W.; Bergstein, D. A.; Gonzalez, R.; Cabodi, M.; Gershoni, J. M.; Goldberg, B. B.; Unlu, M. S. *Proc. Natl. Acad. Sci. U. S. A.* **2008**, *105*, 7988.
(59) Hanel, C.; Gauglitz, G. *Anal. Bioanal. Chem.* **2002**, *372*, 91.
(60) (a) Berggren, C.; Bjarnason, B.; Johansson, G. *Electroanalysis* **2001**, *13*, 173. (b) Chang, B. Y.; Park, S. M. In *Annual Review Analytical Chemistry*; Yeung, E. S., Zare, R. N., Eds.; Annual Reviews: Palo Alto, 2010; Vol. 3.
(61) (a) Moy, V. T.; Florin, E. L.; Gaub, H. E. *Science* **1994**, *266*, 257. (b) Lee, G. U.; Kidwell, D. A.; Colton, R. J. *Langmuir* **1994**, *10*, 354.
(62) Homola, J. *Surface Plasmon Resonance Based Sensors*; Springer Verlag: Berlin, 2006.
(63) Schasfoort, R. B. M.; Tudos, A. J. *Handbook of Surface Plasmon Resonance*; Royal Society of Chemistry: Cambridge, UK, 2008.
(64) Homola, J.; Yee, S. S.; Gauglitz, G. *Sens. Actuators, B* **1999**, *54*, 3.
(65) Abdulhalim, I.; Zourob, M.; Lakhtakia, A. *Electromagnetics* **2008**, *28*, 214.
(66) (a) Chien, F. C.; Chen, S. J. *Biosens. Bioelectron.* **2004**, *20*, 633. (b) Kurosawa, K.; Pierce, R. M.; Ushioda, S.; Hemminger, J. C. *Phys. Rev. B: Condens. Matter Mater. Phys.* **1986**, *33*, 789. (c) Čtyroký, J.; Homola, J.; Lambeck, P. V.; Musa, S.; Hoekstra, H. J. W. M.; Harris, R. D.; Wilkinson, J. S.; Usievich, B.; Lyndin, N. M. *Sens. Actuators, B* **1999**, *54*, 66.
(67) (a) Abbas, A.; Linman, M. J.; Cheng, Q. *Biosens. Bioelectron.* **2011**, *26*, 1815. (b) Barnes, W. L.; Dereux, A.; Ebbesen, T. W. *Nature* **2003**, *424*, 824.
(68) Otto, A. *Z. Phys.* **1968**, *216*, 398.
(69) Kretschmann, E.; Raether, H. *Z. Naturforsch., A: Phys. Sci.* **1968**, *A 23*, 2135.
(70) Schasfoort, R. B. M.; Tudos, A. J. (Eds.) *Handbook of Surface Plasmon Resonance*; Royal Society of Chemistry: Cambridge, UK, 2008.
(71) Sarid, D.; Challener, W. A. *Modern Introduction to Surface Plasmons: Theory, Mathematica Modeling, and Applications*; Cambridge University Press: New York, 2010.
(72) (a) Dostálek, J.; Čtyroký, J.; Homola, J.; Brynda, E.; Skalský, M.; Nekvindová, P.; Špirková, J.; Škvor, J.; Schröfel, J. *Sens. Actuators, B* **2001**, *76*, 8. (b) Toyama, S.; Doumae, N.; Shoji, A.; Ikariyama, Y. *Sens. Actuators, B* **2000**, *65*, 32.
(73) (a) Hoa, X. D.; Kirk, A. G.; Tabrizian, M. *Biosens. Bioelectron.* **2007**, *23*, 151. (b) Suzuki, A.; Kondoh, J.; Matsui, Y.; Shiokawa, S.; Suzuki, K. *Sens. Actuators, B* **2005**, *106*, 383.
(74) Sharma, A. K.; Jha, R.; Gupta, B. D. *IEEE Sens. J.* **2007**, *7*, 1118.
(75) (a) Homola, J.; Koudela, I.; Yee, S. S. *Sens. Actuators, B* **1999**, *54*, 16. (b) Byun, K. M.; Kim, S. J.; Kim, D. *Appl. Opt.* **2007**, *46*, 5703. (c) Singh, B. K.; Hillier, A. C. *Anal. Chem.* **2006**, *78*, 2009. (d) Lee, Y.; Hoshino, K.; Alu, A.; Zhang, X. J. *App. Phys. Lett.* **2012**, *101*, 041102.
(76) Gauvreau, B.; Hassani, A.; Fassi Fehri, M.; Kabashin, A.; Skorobogatiy, M. A. *Opt. Express* **2007**, *15*, 11413.
(77) (a) Sun, B.; Chen, M. Y.; Zhang, Y. K.; Yang, J. C.; Yao, J. Q.; Cui, H. X. *Opt. Express* **2011**, *19*, 4091. (b) Hassani, A.; Skorobogatiy, M. *Opt. Express* **2006**, *14*, 11616.
(78) Russell, P. *Science* **2003**, *299*, 358.
(79) Wang, K.; Zheng, Z.; Su, Y. L.; Wang, Z. Y.; Song, L. S.; Zhu, J. S. *Opt. Express* **2009**, *17*, 4468.
(80) Willets, K. A.; Van Duyne, R. P. *Annu. Rev. Phys. Chem.* **2007**, *58*, 267.
(81) Kelly, K. L.; Coronado, E.; Zhao, L. L.; Schatz, G. C. *J. Phys. Chem. B* **2003**, *107*, 668.
(82) (a) Eustis, S.; El-Sayed, M. A. *Chem. Soc. Rev.* **2006**, *35*, 209. (b) Schultz, S.; Smith, D. R.; Mock, J. J.; Schultz, D. A. *Proc. Natl. Acad. Sci. U. S. A.* **2000**, *97*, 996.
(83) Jung, L. S.; Campbell, C. T.; Chinowsky, T. M.; Mar, M. N.; Yee, S. S. *Langmuir* **1998**, *14*, 5636.
(84) (a) McFarland, A. D.; Van Duyne, R. P. *Nano Lett.* **2003**, *3*, 1057. (b) Mock, J. J.; Smith, D. R.; Schultz, S. *Nano Lett.* **2003**, *3*, 485. (c) Jin, R.; Charles Cao, Y.; Hao, E.; Metraux, G. S.; Schatz, G. C.; Mirkin, C. A. *Nature* **2003**, *425*, 487. (d) Sherry, L. J.; Chang, S. H.; Schatz, G. C.; Van Duyne, R. P.; Wiley, B. J.; Xia, Y. *Nano Lett.* **2005**,

5, 2034. (e) Huang, X.; El-Sayed, I. H.; Qian, W.; El-Sayed, M. A. *J. Am. Chem. Soc.* **2006**, *128*, 2115. (f) Jensen, T. R.; Malinsky, M. D.; Haynes, C. L.; Van Duyne, R. P. *J. Phys. Chem. B* **2000**, *104*, 10549.
(85) Myers, F. B.; Lee, L. P. *Lab Chip* **2008**, *8*, 2015.
(86) Haes, A. J.; Van Duyne, R. P. *Expert Rev. Mol. Diagn.* **2004**, *4*, 527.
(87) Escobedo, C. *Lab Chip* **2013**, *13*, 2445.
(88) Maria, J.; Truong, T. T.; Yao, J. M.; Lee, T. W.; Nuzzo, R. G.; Leyffer, S.; Gray, S. K.; Rogers, J. A. *J. Phys. Chem. C* **2009**, *113*, 10493.
(89) Truong, T. T.; Maria, J.; Yao, J.; Stewart, M. E.; Lee, T. W.; Gray, S. K.; Nuzzo, R. G.; Rogers, J. A. *Nanotechnology* **2009**, *20*, 434011.
(90) Caldwell, J. D.; Glembocki, O.; Bezares, F. J.; Bassim, N. D.; Rendell, R. W.; Feygelson, M.; Ukaegbu, M.; Kasica, R.; Shirey, L.; Hosten, C. *ACS Nano* **2011**, *5*, 4046.
(91) Aksu, S.; Yanik, A. A.; Adato, R.; Artar, A.; Huang, M.; Altug, H. *Nano Lett.* **2010**, *10*, 2511.
(92) Lee, S. W.; Lee, K. S.; Ahn, J.; Lee, J. J.; Kim, M. G.; Shin, Y. B. *ACS Nano* **2011**, *5*, 897.
(93) McPhillips, J.; Murphy, A.; Jonsson, M. P.; Hendren, W. R.; Atkinson, R.; Hook, F.; Zayats, A. V.; Pollard, R. J. *ACS Nano* **2010**, *4*, 2210.
(94) Chung, P. Y.; Lin, T. H.; Schultz, G.; Batich, C.; Jiang, P. *Appl. Phys. Lett.* **2010**, *96*, 261108.
(95) Nathan, C. L.; Prashant, N.; Kevin, M. M.; David, J. N.; Sang-Hyun, O. *Rep. Prog. Phys.* **2012**, *75*, 036501.
(96) van Beijnum, F.; Retif, C.; Smiet, C. B.; Liu, H. T.; Lalanne, P.; van Exter, M. P. *Nature* **2012**, *492*, 411.
(97) (a) Gordon, R.; Sinton, D.; Kavanagh, K. L.; Brolo, A. G. *Acc. Chem. Res.* **2008**, *41*, 1049. (b) Gao, H. W.; Henzie, J.; Odom, T. W. *Nano Lett.* **2006**, *6*, 2104.
(98) (a) Sannomiya, T.; Scholder, O.; Jefimovs, K.; Hafner, C.; Dahlin, A. B. *Small* **2011**, *7*, 1653. (b) Yang, J.-C.; Gao, H.; Suh, J. Y.; Zhou, W.; Lee, M. H.; Odom, T. W. *Nano Lett.* **2010**, *10*, 3173.
(99) Lee, M. H.; Gao, H. W.; Henzie, J.; Odom, T. W. *Small* **2007**, *3*, 2029.
(100) (a) Shuford, K. L.; Ratner, M. A.; Gray, S. K.; Schatz, G. C. *Appl. Phys. B: Lasers Opt.* **2006**, *84*, 11. (b) Stewart, M. E.; Mack, N. H.; Malyarchuk, V.; Soares, J.; Lee, T. W.; Gray, S. K.; Nuzzo, R. G.; Rogers, J. A. *Proc. Natl. Acad. Sci. U. S. A.* **2006**, *103*, 17143. (c) Yao, J.; Le, A.-P.; Gray, S. K.; Moore, J. S.; Rogers, J. A.; Nuzzo, R. G. *Adv. Mater.* **2010**, *22*, 1102. (d) Lesuffleur, A.; Im, H.; Lindquist, N. C.; Oh, S. H. *Appl. Phys. Lett.* **2007**, *90*, 243110.
(101) (a) Escobedo, C.; Brolo, A. G.; Gordon, R.; Sinton, D. *Nano Lett.* **2012**, *12*, 1592. (b) Eftekhari, F.; Escobedo, C.; Ferreira, J.; Duan, X. B.; Girotto, E. M.; Brolo, A. G.; Gordon, R.; Sinton, D. *Anal. Chem.* **2009**, *81*, 4308.
(102) (a) Yang, J.-C.; Ji, J.; Hogle, J. M.; Larson, D. N. *Nano Lett.* **2008**, *8*, 2718. (b) Lindquist, N. C.; Lesuffleur, A.; Im, H.; Oh, S.-H. *Lab Chip* **2009**, *9*, 382. (c) Liu, G.; Doll, J.; Lee, L. *Opt. Express* **2005**, *13*, 8520.
(103) Tetz, K. A.; Pang, L.; Fainman, Y. *Opt. Lett.* **2006**, *31*, 1528.
(104) Im, H.; Sutherland, J. N.; Maynard, J. A.; Oh, S. H. *Anal. Chem.* **2012**, *84*, 1941.
(105) Lee, S. H.; Lindquist, N. C.; Wittenberg, N. J.; Jordan, L. R.; Oh, S. H. *Lab Chip* **2012**, *12*, 3882.
(106) (a) Kim, Y. G.; Moon, S.; Kuritzkes, D. R.; Demirci, U. *Biosens. Bioelectron.* **2009**, *25*, 253. (b) Wang, S.; Esfahani, M.; Gurkan, U. A.; Inci, F.; Kuritzkes, D. R.; Demirci, U. *Lab Chip* **2012**, *12*, 1508.
(107) Yanik, A. A.; Huang, M.; Kamohara, O.; Artar, A.; Geisbert, T. W.; Connor, J. H.; Altug, H. *Nano Lett.* **2010**, *10*, 4962.
(108) (a) Dittrich, P. S.; Manz, A. *Nat. Rev. Drug Discovery* **2006**, *5*, 210. (b) Sun, S.; Yang, M.; Kostov, Y.; Rasooly, A. *Lab Chip* **2010**, *10*, 2093. (c) Wang, S.; Inci, F.; Chaunzwa, T. L.; Ramanujam, A.; Vasudevan, A.; Subramanian, S.; Ip, A. C. F.; Sridharan, B.; Gurkan, U. A.; Demirci, U. *Int. J. Nanomed.* **2012**, *7*, 2591. (d) Ozcan, A.; Demirci, U. *Lab Chip* **2008**, *8*, 98. (e) Wan, Y.; Tan, J.; Asghar, W.; Kim, Y.-t.; Liu, Y.; Iqbal, S. M. *J. Phys. Chem. B* **2011**, *115*, 13891.
(109) Toner, M.; Irimia, D. *Annu. Rev. Biomed. Eng.* **2005**, *7*, 77.
(110) Weigl, B.; Domingo, G.; Labarre, P.; Gerlach, J. *Lab Chip* **2008**, *8*, 1999.
(111) (a) Maerkl, S. J.; Quake, S. R. *Proc. Natl. Acad. Sci. U. S. A.* **2009**, *106*, 18650. (b) Liu, Y.; Adams, J. D.; Turner, K.; Cochran, F. V.; Gambhir, S. S.; Soh, H. T. *Lab Chip* **2009**, *9*, 1033.
(112) Hong, J. W.; Studer, V.; Hang, G.; Anderson, W. F.; Quake, S. R. *Nat. Biotechnol.* **2004**, *22*, 435.
(113) (a) Leach, J.; Mushfique, H.; di Leonardo, R.; Padgett, M.; Cooper, J. *Lab Chip* **2006**, *6*, 735. (b) Terray, A.; Oakey, J.; Marr, D. W. M. *Science* **2002**, *296*, 1841.
(114) MacDonald, M. P.; Neale, S.; Paterson, L.; Richies, A.; Dholakia, K.; Spalding, G. C. *J. Biol. Regul. Homeostatic Agents* **2004**, *18*, 200.
(115) Lee, W. G.; Kim, Y. G.; Chung, B. G.; Demirci, U.; Khademhosseini, A. *Adv. Drug Delivery Rev.* **2010**, *62*, 449.
(116) (a) Homola, J.; Vaisocherova, H.; Dostalek, J.; Piliarik, M. *Methods* **2005**, *37*, 26. (b) Saha, K.; Agasti, S. S.; Kim, C.; Li, X.; Rotello, V. M. *Chem. Rev.* **2012**, *112*, 2739.
(117) Dugas, V.; Elaissari, A.; Chevalier, Y. *Surface Sensitization Techniques and Recognition Receptors Immobilization on Biosensors and Microarrays*; Springer Verlag: Berlin, 2010.
(118) Bhushan, B. *J. Vac. Sci. Technol., B* **2003**, *21*, 2262.
(119) Tsougeni, K.; Koukouvinos, G.; Petrou, P. S.; Tserepi, A.; Kakabakos, S. E.; Gogolides, E. *Anal. Bioanal. Chem.* **2012**, *403*, 2757.
(120) Ahn, C. H.; Choi, J. W.; Beaucage, G.; Nevin, J. H.; Lee, J. B.; Puntambekar, A.; Lee, J. Y. *Proc. IEEE* **2004**, *92*, 154.
(121) Wang, S.; Esfahani, M.; Gurkan, U. A.; Inci, F.; Kuritzkes, D. R.; Demirci, U. *Lab Chip* **2012**, *12*, 1508.
(122) Chaki, N. K.; Aslam, M.; Sharma, J.; Vijayamohanan, K. *Proceedings of the Indian Academy of Sciences-Chemical Sciences* **2001**, *113*, 659.
(123) Yourdshahyan, Y.; Zhang, H. K.; Rappe, A. M. *Phys. Rev. B* **2001**, *63*, 081405.
(124) Fischer, M. J. E. *Amine Coupling Through EDC/NHS: A Practical Approach*; Springer Verlag: Berlin, 2010.
(125) (a) Brockman, J. M.; Frutos, A. G.; Corn, R. M. *J. Am. Chem. Soc.* **1999**, *121*, 8044. (b) D'Agata, R.; Corradini, R.; Grasso, G.; Marchelli, R.; Spoto, G. *ChemBioChem* **2008**, *9*, 2067. (c) Fang, S.; Lee, H. J.; Wark, A. W.; Corn, R. M. *J. Am. Chem. Soc.* **2006**, *128*, 14044.
(126) (a) Seed, B. In *Current Protocols in Cell Biology*; John Wiley & Sons, Inc.: New York, 2001. (b) Howarter, J. A.; Youngblood, J. P. *Langmuir* **2006**, *22*, 11142. (c) Lambert, A. G.; Neivandt, D. J.; McAloney, R. A.; Davies, P. B. *Langmuir* **2000**, *16*, 8377. (d) Weetall, H. H. *Appl. Biochem. Biotechnol.* **1993**, *41*, 157. (e) London, G.; Carroll, G. T.; Feringa, B. L. *Org. Biomol. Chem.* **2013**, *11*, 3477.
(127) (a) Moon, S.; Gurkan, U. A.; Blander, J.; Fawzi, W. W.; Aboud, S.; Mugusi, F.; Kuritzkes, D. R.; Demirci, U. *PLoS One* **2011**, *6*, e21409. (b) Kim, Y.-G.; Moon, S.; Kuritzkes, D. R.; Demirci, U. *Biosens. Bioelectron.* **2009**, *25*, 253. (c) Moon, S.; Keles, H. O.; Ozcan, A.; Khademhosseini, A.; Haeggstrom, E.; Kuritzkes, D.; Demirci, U. *Biosens. Bioelectron.* **2009**, *24*, 3208. (d) Cheng, X.; Irimia, D.; Dixon, M.; Sekine, K.; Demirci, U.; Zamir, L.; Tompkins, R. G.; Rodriguez, W.; Toner, M. *Lab Chip* **2007**, *7*, 170. (e) Cheng, X.; Irimia, D.; Dixon, M.; Ziperstein, J. C.; Demirci, U.; Zamir, L.; Tompkins, R. G.; Toner, M.; Rodriguez, W. R. *JAIDS, J. Acquired Immune Defic. Syndr.* **2007**, *45*, 257.
(128) (a) Jung, L. S.; Nelson, K. E.; Stayton, P. S.; Campbell, C. T. *Langmuir* **2000**, *16*, 9421. (b) Nelson, K. E.; Gamble, L.; Jung, L. S.; Boeckl, M. S.; Naeemi, E.; Golledge, S. L.; Sasaki, T.; Castner, D. G.; Campbell, C. T.; Stayton, P. S. *Langmuir* **2001**, *17*, 2807.
(129) Sevimli, S.; Inci, F.; Zareie, H. M.; Bulmus, V. *Biomacromolecules* **2012**, *13*, 3064.
(130) (a) Yuan, J.; Oliver, R.; Li, J.; Lee, J.; Aguilar, M.; Wu, Y. *Biosens. Bioelectron.* **2007**, *23*, 144. (b) Diaz-Mochon, J. J.; Tourniaire, G.; Bradley, M. *Chem. Soc. Rev.* **2007**, *36*, 449.
(131) Chivers, C. E.; Crozat, E.; Chu, C.; Moy, V. T.; Sherratt, D. J.; Howarth, M. *Nat. Methods* **2010**, *7*, 391.

(132) (a) Inoshima, Y.; Shimizu, S.; Minamoto, N.; Hirai, K.; Sentsui, H. *Clin. Diagn. Lab. Immunol.* **1999**, *6*, 388. (b) Chackerian, B.; Briglio, L.; Albert, P. S.; Lowy, D. R.; Schiller, J. T. *J. Virol.* **2004**, *78*, 4037. (c) Onen, O.; Ahmad, A. A.; Guldiken, R.; Gallant, N. D. *Sensors* **2012**, *12*, 12317.
(133) (a) Steel, A. B.; Levicky, R. L.; Herne, T. M.; Tarlov, M. J. *Biophys. J.* **2000**, *79*, 975. (b) Nieba, L.; NiebaAxmann, S. E.; Persson, A.; Hamalainen, M.; Edebratt, F.; Hansson, A.; Lidholm, J.; Magnusson, K.; Karlsson, A. F.; Pluckthun, A. *Anal. Biochem.* **1997**, *252*, 217.
(134) Nogues, C.; Leh, H.; Lautru, J.; Delelis, O.; Buckle, M. *PLoS One* **2012**, *7*, e44287.
(135) Arlett, J. L.; Myers, E. B.; Roukes, M. L. *Nat. Nanotechnol.* **2011**, *6*, 203.
(136) Thipmanee, O.; Samanman, S.; Sankoh, S.; Numnuam, A.; Limbut, W.; Kanatharana, P.; Vilaivan, T.; Thavarungkul, P. *Biosens. Bioelectron.* **2012**, *38*, 430.
(137) Vogt, R. F.; Phillips, D. L.; Henderson, L. O.; Whitfield, W.; Spierto, F. W. *J. Immunol. Methods* **1987**, *101*, 43.
(138) Lakshmipriya, T.; Fujimaki, M.; Gopinath, S. C. B.; Awazu, K.; Horiguchi, Y.; Nagasaki, Y. *Analyst* **2013**, *138*, 2863.
(139) Nagasaki, Y. *Polym. J.* **2011**, *43*, 949.
(140) Uchida, K.; Otsuka, H.; Kaneko, M.; Kataoka, K.; Nagasaki, Y. *Anal. Chem.* **2005**, *77*, 1075.
(141) Durmus, N. G.; Taylor, E. N.; Inci, F.; Kummer, K. M.; Tarquinio, K. M.; Webster, T. J. *Int. J. Nanomed.* **2012**, *7*, 537.
(142) (a) Beeram, S. R.; Zamborini, F. P. *J. Am. Chem. Soc.* **2009**, *131*, 11689. (b) Dahlin, A. B.; Wittenberg, N. J.; Höök, F.; Oh, S.-H. *Nanophotonics* **2013**, *2*, 83. (c) Lee, Y. K.; Lee, H.; Nam, J.-M. *NPG Asia Mater.* **2013**, *5*.
(143) Cooper, M. A. *J. Mol. Recognit.* **2004**, *17*, 286.
(144) Jonsson, M. P.; Jonsson, P.; Dahlin, A. B.; Hook, F. *Nano Lett.* **2007**, *7*, 3462.
(145) (a) Pera, I.; Fritz, J. *Langmuir* **2007**, *23*, 1543. (b) Lee, M.; Park, J. E.; Park, C.; Choi, H. C. *Langmuir* **2013**, *29*, 9967.
(146) Baciu, C. L.; Becker, J.; Janshoff, A.; Soennichsen, C. *Nano Lett.* **2008**, *8*, 1724.
(147) Wu, H.-J.; Henzie, J.; Lin, W.-C.; Rhodes, C.; Li, Z.; Sartorel, E.; Thorner, J.; Yang, P.; Groves, J. T. *Nat. Methods* **2012**, *9*, 1189.
(148) Yang, Y.-H.; Nam, J.-M. *Anal. Chem.* **2009**, *81*, 2564.
(149) (a) Cuiffi, J.; Soong, R.; Manolakos, S.; Mohapatra, S.; Larson, D. In *26th Southern Biomedical Engineering Conference SBEC 2010*, April 30−May 2, 2010, College Park, MD; Herold, K., Vossoughi, J., Bentley, W., Eds.; Springer: Berlin, 2010; Vol. *32* (b) Dahlin, A. B.; Jonsson, M. P.; Hook, F. *Adv. Mater.* **2008**, *20*, 1436. (c) Im, H.; Lesuffleur, A.; Lindquist, N. C.; Oh, S.-H. *Anal. Chem.* **2009**, *81*, 2854.
(150) Yusko, E. C.; Johnson, J. M.; Majd, S.; Prangkio, P.; Rollings, R. C.; Li, J.; Yang, J.; Mayer, M. *Nat. Nanotechnol.* **2011**, *6*, 253.
(151) Jeong, H.-J.; Pyun, W.-H.; Yang, S. Y. *Macromol. Rapid Commun.* **2009**, *30*, 1109.
(152) Toma, M.; Jonas, U.; Mateescu, A.; Knoll, W.; Dostalek, J. *J. Phys. Chem. C* **2013**, *117*, 11705.
(153) Gurkan, U. A.; Tasoglu, S.; Akkaynak, D.; Avci, O.; Unluisler, S.; Canikyan, S.; MacCallum, N.; Demirci, U. *Advanced Healthcare Materials* **2012**, *1* (5), 661 DOI: 10.1002/adhm.201200009.
(154) Gurkan, U. A.; Anand, T.; Tas, H.; Elkan, D.; Akay, A.; Keles, H. O.; Demirci, U. *Lab Chip* **2011**, *11* (23), 3979.
(155) (a) Love, J. C.; Estroff, L. A.; Kriebel, J. K.; Nuzzo, R. G.; Whitesides, G. M. *Chem. Rev.* **2005**, *105*, 1103. (b) Gan, W.; Xu, B.; Dai, H.-L. *Angew. Chem., Int. Ed.* **2011**, *50*, 6622.
(156) Bain, C. D.; Troughton, E. B.; Tao, Y. T.; Evall, J.; Whitesides, G. M.; Nuzzo, R. G. *J. Am. Chem. Soc.* **1989**, *111*, 321.
(157) Hostetler, M. J.; Templeton, A. C.; Murray, R. W. *Langmuir* **1999**, *15*, 3782.
(158) Feuz, L.; Jonsson, P.; Jonsson, M. P.; Hook, F. *ACS Nano* **2010**, *4*, 2167.
(159) Jemal, A.; Bray, F.; Center, M. M.; Ferlay, J.; Ward, E.; Forman, D. *Ca-Cancer J. Clin.* **2011**, *61*, 69.
(160) American Cancer Society. *Global Cancer Facts & Figures*, 2nd ed.; http://www.cancer.org/acs/groups/content/@epidemiologysurveilance/documents/document/acspc-027766.pdf, accessed on Sept 1, 2013.
(161) World Cancer Research Fund International. *Cancer Statistics: Data Comparing More and Less Developed Countries*; WCRF: London, 2013.
(162) Rizvi, I.; Gurkan, U. A.; Tasoglu, S.; Alagic, N.; Celli, J. P.; Mensah, L. B.; Mai, Z.; Demirci, U.; Hasan, T. *Proc. Natl. Acad. Sci. U. S. A.* **2013**, *110*, E1974.
(163) Wang, L.; Asghar, W.; Demirci, U.; Wan, Y. *Nano Today* **2013**, *8*, 374.
(164) (a) Xie, K. P. *Cytokine Growth Factor Rev.* **2001**, *12*, 375. (b) Watanabe, H.; Iwase, M.; Ohashi, M.; Nagumo, M. *Oral Oncol.* **2002**, *38*, 670.
(165) St. John, M. A. R.; Li, Y.; Zhou, X. F.; Denny, P.; Ho, C. M.; Montemagno, C.; Shi, W. Y.; Qi, F. X.; Wu, B.; Sinha, U.; Jordan, R.; Wolinsky, L.; Park, N. H.; Liu, H. H.; Abemayor, E.; Wong, D. T. W. *Arch. Otolaryngol., Head Neck Surg.* **2004**, *130*, 929.
(166) Yang, C. Y.; Brooks, E.; Li, Y.; Denny, P.; Ho, C. M.; Qi, F. X.; Shi, W. Y.; Wolinsky, L.; Wu, B.; Wong, D. T. W.; Montemagno, C. D. *Lab Chip* **2005**, *5*, 1017.
(167) (a) Diamandis, E. P. *Trends Endocrinol. Metab.* **1998**, *9*, 310. (b) Brawer, M. K.; Lange, P. H. *World J. Urol.* **1989**, *7*, 7.
(168) Black, M. H.; Giai, M.; Ponzone, R.; Sismondi, P.; Yu, H.; Diamandis, E. P. *Clin. Cancer. Res.* **2000**, *6*, 467.
(169) Cho, J.-W.; Kang, D.-Y.; Jang, Y.-H.; Kim, H.-H.; Min, J.; Oh, B.-K. *Colloids Surf., A* **2008**, *313*, 655.
(170) Uludag, Y.; Tothill, I. E. *Anal. Chem.* **2012**, *84*, 5898.
(171) Fernandez, F.; Hegnerova, K.; Piliarik, M.; Sanchez-Baeza, F.; Homola, J.; Marco, M. P. *Biosens. Bioelectron.* **2010**, *26*, 1231.
(172) Feltis, B. N.; Sexton, B. A.; Glenn, F. L.; Best, M. J.; Wilkins, M.; Davis, T. J. *Biosens. Bioelectron.* **2008**, *23*, 1131.
(173) Kurita, R.; Yokota, Y.; Sato, Y.; Mizutani, F.; Niwa, O. *Anal. Chem.* **2006**, *78*, 5525.
(174) Chinowsky, T. M.; Soelberg, S. D.; Baker, P.; Swanson, N. R.; Kauffman, P.; Mactutis, A.; Grow, M. S.; Atmar, R.; Yee, S. S.; Furlong, C. E. *Biosens. Bioelectron.* **2007**, *22*, 2268.
(175) (a) Englebienne, P. *Analyst* **1998**, *123*, 1599. (b) Hall, W. P.; Anker, J. N.; Lin, Y.; Modica, J.; Mrksich, M.; Van Duyne, R. P. *J. Am. Chem. Soc.* **2008**, *130*, 5836.
(176) (a) Sonnichsen, C.; Reinhard, B. M.; Liphardt, J.; Alivisatos, A. P. *Nat. Biotechnol.* **2005**, *23*, 741. (b) Sota, H.; Hasegawa, Y.; Iwakura, M. *Anal. Chem.* **1998**, *70*, 2019.
(177) Love, J. C.; Estroff, L. A.; Kriebel, J. K.; Nuzzo, R. G.; Whitesides, G. M. *Chem Rev* **2005**, *105*, 1103.
(178) Hutter, E.; Fendler, J. H. *Adv. Mater.* **2004**, *16*, 1685.
(179) (a) Elghanian, R.; Storhoff, J. J.; Mucic, R. C.; Letsinger, R. L.; Mirkin, C. A. *Science* **1997**, *277*, 1078. (b) Storhoff, J. J.; Elghanian, R.; Mucic, R. C.; Mirkin, C. A.; Letsinger, R. L. *J. Am. Chem. Soc.* **1998**, *120*, 1959. (c) Taton, T. A.; Mirkin, C. A.; Letsinger, R. L. *Science* **2000**, *289*, 1757.
(180) Reinhard, B. M.; Siu, M.; Agarwal, H.; Alivisatos, A. P.; Liphardt, J. *Nano Lett.* **2005**, *5*, 2246.
(181) Haynes, C. L.; Van Duyne, R. P. *J. Phys. Chem. B* **2001**, *105*, 5599.
(182) Xiang, G.; Zhang, N.; Zhou, X. *Nanoscale Res. Lett.* **2010**, *5*, 818.
(183) Haes, A. J.; Chang, L.; Klein, W. L.; Van Duyne, R. P. *J. Am. Chem. Soc.* **2005**, *127*, 2264.
(184) Endo, T.; Kerman, K.; Nagatani, N.; Takamura, Y.; Tamiya, E. *Anal. Chem.* **2005**, *77*, 6976.
(185) (a) Kim, D.-K.; Kerman, K.; Saito, M.; Sathuluri, R. R.; Endo, T.; Yamamura, S.; Kwon, Y.-S.; Tamiya, E. *Anal. Chem.* **2007**, *79*, 1855. (b) Hutter, E.; Pileni, M.-P. *J. Phys. Chem. B* **2003**, *107*, 6497.
(186) (a) Marinakos, S. M.; Chen, S.; Chilkoti, A. *Anal. Chem.* **2007**, *79*, 5278. (b) Nusz, G. J.; Marinakos, S. M.; Curry, A. C.; Dahlin, A.; Hook, F.; Wax, A.; Chilkoti, A. *Anal. Chem.* **2008**, *80*, 984.

(187) Kim, D.-K.; Kerman, K.; Hiep, H. M.; Saito, M.; Yamamura, S.; Takamura, Y.; Kwon, Y.-S.; Tamiya, E. *Anal. Biochem.* **2008**, *379*, 1.
(188) Singh, A. K.; Senapati, D.; Wang, S.; Griffin, J.; Neely, A.; Candice, P.; Naylor, K. M.; Varisli, B.; Kalluri, J. R.; Ray, P. C. *ACS Nano* **2009**, *3*, 1906.
(189) Truong, P. L.; Kim, B. W.; Sim, S. J. *Lab Chip* **2012**, *12*, 1102.
(190) Zhou, W.; Ma, Y.; Yang, H.; Ding, Y.; Luo, X. *Int. J. Nanomedicine* **2011**, *6*, 381.
(191) Duan, R. Q.; Yuan, J. L.; Yang, H.; Luo, X. G.; Xi, M. R. *Neoplasma* **2012**, *59*, 348.
(192) El-Sayed, I. H.; Huang, X.; El-Sayed, M. A. *Nano Lett.* **2005**, *5*, 829.
(193) Endo, T.; Kerman, K.; Nagatani, N.; Hiepa, H. M.; Kim, D.-K.; Yonezawa, Y.; Nakano, K.; Tamiya, E. *Anal. Chem.* **2006**, *78*, 6465.
(194) Huang, C.; Bonroy, K.; Reekmans, G.; Laureyn, W.; Verhaegen, K.; De Vlaminck, I.; Lagae, L.; Borghs, G. *Biomed. Microdevices* **2009**, *11*, 893.
(195) Rothenhausler, B.; Knoll, W. *Nature* **1988**, *332*, 615.
(196) (a) Steiner, G. *Anal. Bioanal. Chem.* **2004**, *379*, 328. (b) Thiel, A. J.; Frutos, A. G.; Jordan, C. E.; Corn, R. M.; Smith, L. M. *Anal. Chem.* **1997**, *69*, 4948.
(197) (a) Jordan, C. E.; Corn, R. M. *Anal. Chem.* **1997**, *69*, 1449. (b) Lee, H. J.; Goodrich, T. T.; Corn, R. M. *Anal. Chem.* **2001**, *73*, 5525. (c) Piscevic, D.; Lawall, R.; Veith, M.; Liley, M.; Okahata, Y.; Knoll, W. *Appl. Surf. Sci.* **1995**, *90*, 425. (d) Jordan, C. E.; Frutos, A. G.; Thiel, A. J.; Corn, R. M. *Anal. Chem.* **1997**, *69*, 4939. (e) Brockman, J. M.; Frutos, A. G.; Corn, R. M. *J. Am. Chem. Soc.* **1999**, *121*, 8044. (f) Nelson, B. P.; Frutos, A. G.; Brockman, J. M.; Corn, R. M. *Anal. Chem.* **1999**, *71*, 3928. (g) Brockman, J. M.; Nelson, B. P.; Corn, R. M. *Annu. Rev. Phys. Chem.* **2000**, *51*, 41. (h) Wegner, G. J.; Wark, A. W.; Lee, H. J.; Codner, E.; Saeki, T.; Fang, S.; Corn, R. M. *Anal. Chem.* **2004**, *76*, 5677. (i) Fang, S.; Lee, H. J.; Wark, A. W.; Kim, H. M.; Corn, R. M. *Anal. Chem.* **2005**, *77*, 6528. (j) Lee, H. J.; Li, Y.; Wark, A. W.; Corn, R. M. *Anal. Chem.* **2005**, *77*, 5096. (k) Wark, A. W.; Lee, H. J.; Corn, R. M. *Anal. Chem.* **2005**, *77*, 3904. (l) Lee, H. J.; Wark, A. W.; Corn, R. M. *Langmuir* **2006**, *22*, 5241.
(198) (a) Wegner, G. J.; Lee, H. J.; Corn, R. M. *Anal. Chem.* **2002**, *74*, 5161. (b) Smith, E. A.; Thomas, W. D.; Kiessling, L. L.; Corn, R. M. *J. Am. Chem. Soc.* **2003**, *125*, 6140. (c) Smith, E. A.; Corn, R. M. *Appl. Spectrosc.* **2003**, *57*, 320A. (d) Lee, H. J.; Wark, A. W.; Li, Y.; Corn, R. M. *Anal. Chem.* **2005**, *77*, 7832. (e) Wegner, G. J.; Lee, H. J.; Marriott, G.; Corn, R. M. *Anal. Chem.* **2003**, *75*, 4740.
(199) Nelson, B. P.; Grimsrud, T. E.; Liles, M. R.; Goodman, R. M.; Corn, R. M. *Anal. Chem.* **2001**, *73*, 1.
(200) (a) Goodrich, T. T.; Lee, H. J.; Corn, R. M. *Anal. Chem.* **2004**, *76*, 6173. (b) Goodrich, T. T.; Lee, H. J.; Corn, R. M. *J. Am. Chem. Soc.* **2004**, *126*, 4086.
(201) Baute, J.; Depicker, A. *Crit. Rev. Biochem. Mol. Biol.* **2008**, *43*, 239.
(202) Corne, C.; Fiche, J.-B.; Gasparutto, D.; Cunin, V.; Suraniti, E.; Buhot, A.; Fuchs, J.; Calemczuk, R.; Livache, T.; Favier, A. *Analyst* **2008**, *133*, 1036.
(203) Li, Y.; Lee, H. J.; Corn, R. M. *Nucleic Acids Res.* **2006**, *34*, 6416.
(204) Li, Y.; Lee, H. J.; Corn, R. M. *Anal. Chem.* **2007**, *79*, 1082.
(205) Wang, Z.; Wilkop, T.; Xu, D.; Dong, Y.; Ma, G.; Cheng, Q. *Anal. Bioanal. Chem.* **2007**, *389*, 819.
(206) (a) Shumaker-Parry, J. S.; Campbell, C. T. *Anal. Chem.* **2004**, *76*, 907. (b) Shumaker-Parry, J. S.; Aebersold, R.; Campbell, C. T. *Anal. Chem.* **2004**, *76*, 2071.
(207) Campbell, C. T.; Kim, G. *Biomaterials* **2007**, *28*, 2380.
(208) (a) Fu, E.; Foley, J.; Yager, P. *Rev. Sci. Instrum.* **2003**, *74*, 3182. (b) Fu, E.; Chinowsky, T.; Foley, J.; Weinstein, J.; Yager, P. *Rev. Sci. Instrum.* **2004**, *75*, 2300.
(209) (a) Piliarik, M.; Vaisocherová, H.; Homola, J. *Biosens. Bioelectron.* **2005**, *20*, 2104. (b) Piliarik, M.; Vaisocherová, H.; Homola, J. *Sens. Actuators, B* **2007**, *121*, 187.
(210) Lee, K.-H.; Su, Y.-D.; Chen, S.-J.; Tseng, F.-G.; Lee, G.-B. *Biosens. Bioelectron.* **2007**, *23*, 466.
(211) Usui-Aoki, K.; Shimada, K.; Nagano, M.; Kawai, M.; Koga, H. *Proteomics* **2005**, *5*, 2396.
(212) Kyo, M.; Usui-Aoki, K.; Koga, H. *Anal. Chem.* **2005**, *77*, 7115.
(213) Kanda, V.; Kariuki, J. K.; Harrison, D. J.; McDermott, M. T. *Anal. Chem.* **2004**, *76*, 7257.
(214) Lee, H. J.; Nedelkov, D.; Corn, R. M. *Anal. Chem.* **2006**, *78*, 6504.
(215) Luo, Y.; Yu, F.; Zare, R. N. *Lab Chip* **2008**, *8*, 694.
(216) Wu, H.; Huang, B.; Zare, R. N. *Lab Chip* **2005**, *5*, 1393.
(217) Ouellet, E.; Lausted, C.; Lin, T.; Yang, C. W. T.; Hood, L.; Lagally, E. T. *Lab Chip* **2010**, *10*, 581.
(218) Wang, S.; Shan, X.; Patel, U.; Huang, X.; Lu, J.; Li, J.; Tao, N. *Proc. Natl. Acad. Sci. U. S. A.* **2010**, *107*, 16028.
(219) *The Convergence of Life Sciences, Physical Sciences, and Engineering*; http://dc.mit.edu/sites/dc.mit.edu/files/MIT%20White%20Paper%20on%20Convergence.pdf, accessed on Sept 1, 2013.
(220) *NIH Research Timelines*; http://report.nih.gov/nihfactsheets/ViewFactSheet.aspx?csid=112, accessed on Sept 1, 2013.
(221) Peeling, R. W.; Mabey, D.; Herring, A.; Hook, E. W. *Nat. Rev. Micro.* **2006**, *4*, 909.
(222) Gervais, L.; de Rooij, N.; Delamarche, E. *Adv. Mater.* **2011**, *23*, H151.
(223) Savage, N. *Nat. Photonics* **2009**, *3*, 601.
(224) Stewart, M. E.; Anderton, C. R.; Thompson, L. B.; Maria, J.; Gray, S. K.; Rogers, J. A.; Nuzzo, R. G. *Chem. Rev.* **2008**, *108*, 494.
(225) Wang, S.; Zhao, X.; Khimji, I.; Akbas, R.; Qiu, W.; Edwards, D.; Cramer, D. W.; Ye, B.; Demirci, U. *Lab Chip* **2011**, *11* (20), 3411.
(226) Wang, S.; Tasoglu, S.; Chen, P. Z.; Chen, M.; Akbas, R.; Wach, S.; Ozdemir, C. I.; Gurkan, U. A.; Giguel, F. F.; Kuritzkes, D. R.; Demirci, U. *Sci. Rep.* **2014**, *4*, 3796.
(227) Gallegos, D.; Long, K. D.; Yu, H.; Clark, P. P.; Lin, Y.; George, S.; Natha, P.; Cunningham, B. T. *Lab Chip* **2013**, *13*, 2124.